production of cytokines such as type I and type III IFNs.[5] RIG-I is activated through recognition of short double-strand RNA (dsRNA) or triphosphate at the 5′ end of dsRNA as pathogen-associated molecular patterns,[6,7] forming a homo-oligomer that binds with the caspase recruitment domain (CARD) of Cardif (also known as MAVS, VISA, or IPS-1).[8-11] Cardif subsequently recruits TANK binding kinase 1 (TBK1) and IκB kinase ϵ (IKKϵ) kinases, which catalyze phosphorylation and activation of IFN regulatory factor-3 (IRF-3).[12] Activation of TBK1 and IKKϵ results in the phosphorylation of IRF-3 or IRF-7, translocation to the nucleus, and induction of IFN-β mRNA transcription.

Several HCV proteins can block host cellular antiviral responses. HCV core protein blocks IFN signaling by interacting with signal transducer and activator of transcription protein-1 (STAT1).[13] The core protein also induces expression of suppressor of cytokine signaling-1 (SOCS1) and SOCS3, and blocks Janus kinase–STAT signaling.[14,15] A well-elucidated immune evasion strategy of HCV involves NS3/4A serine protease and its ability to inhibit host IFN signal pathways. Gale and colleagues[11,16,17] revealed that NS3/4A protease cleaves Cardif at Cys-508 resulting in dislocation of Cardif from mitochondria, and blocks downstream signaling of IFN-β production. On the other hand, Baril et al.[18] reported that Cardif was still able to form a homo-oligomer and to activate downstream IFN production signaling despite delocalization from the mitochondria. These reports suggest that homo-oligomerization of Cardif, and not mitochondrial anchorage, is essential for the activation of downstream IFN signaling and that other virus-derived molecules may cooperate with NS3/4A to abrogate the signaling of IFN production.

We reported previously that HCV-NS4B, as well as NS3/4A, inhibited RIG-I and Cardif-mediated interferon-stimulated response element (ISRE) activation, while TBK1- and IKKϵ-mediated ISRE activation were not suppressed.[19] These results indicate that NS4B suppresses IFN production signaling by targeting Cardif or other unknown signaling molecules between the level of Cardif and TBK1/IKKϵ.

Recently, a stimulator of interferon genes (STING, also known as MITA/ERIS/MPYS/TMEM173) was identified as a positive regulator of RIG-I–mediated IFN-β signaling.[20-23] STING is a 42-kDa protein localized predominantly in the endoplasmic reticulum (ER) that binds RIG-I, Cardif, TBK1, and IKKϵ. STING is thought to act as a scaffold for Cardif/TBK1/IRF-3 complex upon viral infection.[22] It has been reported that NS4B of yellow fever virus, which is a member of the flaviviridae family of viruses, inhibits its STING activation probably through a direct molecular interaction.[24] These reports have led us postulate that HCV-NS4B may also inhibit RIG-I dependent IFN signaling through association with STING.

In the present study, we further investigated the molecular mechanisms by which HCV-NS4B protein inhibits RIG-I–mediated IFN expression signaling. We demonstrated that HCV-NS4B specifically binds STING, blocks the molecular interaction between STING and Cardif, and suppresses the RIG-I–like receptor–induced activation of IFN-β production signaling.

## Materials and Methods

***Plasmids.*** The ΔRIG-I and RIG-IKA plasmids express constitutively active and inactive RIG-I, respectively.[5] Full-length Cardif (Cardif) and CARD-truncated Cardif (ΔCARD) plasmids were provided by J. Tschopp.[11] Plasmids expressing STING were provided by G. N. Barber.[20] Plasmids expressing HCV NS3/4A, NS4B, and truncated NS4B have been described.[25] Plasmid pIFNβ-Fluc was provided by R. Lin.[26]

***Cell Culture.*** HEK293T and Huh7 cells were maintained in Dulbecco's modified minimal essential medium (Sigma) supplemented with 2 mM L-glutamine and 10% fetal calf serum at 37°C with 5% $CO_2$.

***HCV Replicon Constructs and HCV-JFH1 Cell Culture.*** An HCV subgenomic replicon plasmid, pRep-Feo, expressed fusion protein of firefly luciferase and neomycin phosphotransferase.[27,28] Huh7 cells were transfected by Rep-Feo RNA, cultured in the presence of 500 μg/mL of G418, and a cell line that stably expressed Feo replicon was established. For HCV cell culture, the HCV-JFH1 strain was used.[29,30]

***Antibodies.*** Antibodies used were anti–IRF-3 (FL-425, Santa Cruz Biotechnology), anti-HA (Invitrogen), anti-myc (Invitrogen), mouse anti-PDI (Abcam),

*Address reprint requests to: Naoya Sakamoto, M.D., Ph.D., Department of Gastroenterology and Hepatology, Hokkaido University, Kita15, Nishi8, Kita-ku, Sapporo, Hokkaido, 060-0808, Japan. E-mail: nsakamoto.gast@tmd.ac.jp; fax (81)-11-706-8036.*



*View this article online at wileyonlinelibrary.com.*

*DOI 10.1002/hep.26017*

*Potential conflict of interest: Nothing to report.*

*Additional Supporting Information may be found in the online version of this article.*

rabbit anti-PDI (Enzo Life Science), anti-Flag (Sigma Aldrich), anti-Cardif (Enzo Life Science), anti-phospho–IRF-3 (Ser396, Millipore), anti-monomeric Kusabira-Green C- or N-terminal fragment (MBL), and anti-FACL4 (Abgent).

***Luciferase Reporter Assay.*** IFN-$\beta$ reporter assays were performed as described.[19,31] The plasmids pIFN-$\beta$-Fluc and pRL-CMV were cotransfected with NS3/4A or NS4B, and ΔRIG-I, Cardif, STING or poly(deoxyadenylic-deoxythymidylic) acid [poly(dA:dT)] (Invivogen). RIG-IKA, ΔCARD, and pcDNA3.1, respectively, were used as controls. Luciferase assays were performed 24 hours after transfection by using a 1420 Multilabel Counter (ARVO MX PerkinElmer) and Dual Luciferase Assay System (Promega). Assays were performed in triplicate, and the results are expressed as the mean ± SD.

***Immunoblotting.*** Preparation of total cell lysates was performed as described.[19,28] Protein was separated using NuPAGE 4%-12% Bis/Tris gels (Invitrogen) and blotted onto an Immobilon polyvinylidene difluoride membrane. The membrane was immunoblotted with primary followed by secondary antibody, and protein was detected by chemiluminescence.

***Immunoprecipitation Assay.*** HEK-293T or Huh7 cells were transfected with plasmids as indicated. Twenty-four hours after transfection, cellular proteins were harvested and immunoprecipitation assays were performed using an Immunoprecipitation Kit according to the manufacturer's protocol (Roche Applied Science). The immunoprecipitated proteins were analyzed by immunoblotting.

***Indirect Immunofluorescence Assay.*** Cells seeded onto tissue culture chamber slides were transfected with plasmids as indicated. Twenty-four hours after transfection, the cells were fixed with cold acetone and incubated with primary antibody and subsequently with Alexa488- or Alexa568-labeled secondary antibodies. Mitochondria were stained by MitoTracker (Invitrogen). Cells were visualized using a confocal laser microscope (Fluoview FV10, Olympus).

***BiFC Assay.*** Expression plasmids of NS4B, Cardif, or STING that was fused with N- or C-terminally truncated monomeric Kusabira-Green (mKG) were constructed by inserting polymerase chain reaction–amplified fragments encoding NS4B, Cardif, or STING, respectively, inserted into fragmented mKG vector (Coral Hue Fluo-Chase Kit; MBL). HEK293T cells were transfected with a complementary pair of mKG fusion plasmids. Twenty-four hours after transfection, fluorescence-positive cells were detected and counted by flow cytometry, or observed by confocal laser microscopy.

***Small Interfering RNA Assay.*** Nucleotide sequences of STING-targeted small interfering RNAs (siRNAs) were as follows: (1) 5′-gcaacagcatctatgagcttctggagaac-3′, (2) 5′- gtgcagtgagccagcggctgtatattctc;-3′, (3) 5′-gctggcat ggtcatattacatcggatatc-3′.[22] Stealth RNAi Negative Control Duplex (Medium GC Duplex, Invitrogen) was used. Forty-eight hours after siRNA transfection, expression levels of STING were detected by immunoblotting.

***Statistical Analyses.*** Statistical analyses were performed using unpaired, two-tailed Student $t$ test. $P < 0.05$ were considered to be statistically significant.

## Results

***NS4B Suppressed RIG-I, Cardif, and STING-Mediated Activation of IFN-β Expression Signaling.*** First, we performed a reporter assay using a luciferase reporter plasmid regulated by native IFN-$\beta$ promoter. Consistent with our previous study,[19] overexpression of NS4B, as well as NS3/4A, inhibited the IFN-$\beta$ promoter activation that was induced by ΔRIG-I and Cardif, respectively (Fig. 1A). We next studied whether NS4B targets STING and inhibits RIG-I pathway–mediated activation of IFN-$\beta$ production. Expression of NS4B protein significantly suppressed STING-mediated activation of the IFN-$\beta$ promoter reporter, whereas expression of NS3/4A showed no effect on STING-induced IFN-$\beta$ promoter activity (Fig. 1A). To study whether NS4B blocks the STING-mediated DNA-sensing pathway, we performed a reporter assay using a luciferase reporter plasmid cotransfection with poly(dA:dT), which is a synthetic analog of B-DNA and has been reported to induce STING-mediated IFN-$\beta$ production and NS4B. NS4B significantly blocked poly(dA:dT)-induced IFN-$\beta$ promoter activation, suggesting that NS4B may block STING signaling in the DNA-sensing pathway (Fig. 1A).

Activation of RIG-I signaling induces phosphorylation of IRF-3, which is a hallmark of IRF-3 activation.[32] Thus, we examined the effects of NS3/4A and NS4B expression on phosphorylation of IRF-3 by immunoblotting analysis. As shown in Fig. 1B, overexpression of ΔRIG-I, Cardif, or STING in HEK293T cells increased levels of phosphorylated IRF-3 (pIRF-3). Expression of NS4B impaired the IRF-3 phosphorylation that was induced by ΔRIG-I, Cardif, or STING. NS3/4A also blocked production of pIRF-3 induced by ΔRIG-I or Cardif. Intriguingly, NS3/4A did not block STING-induced pIRF-3 production. These results demonstrate that both NS3/4A and

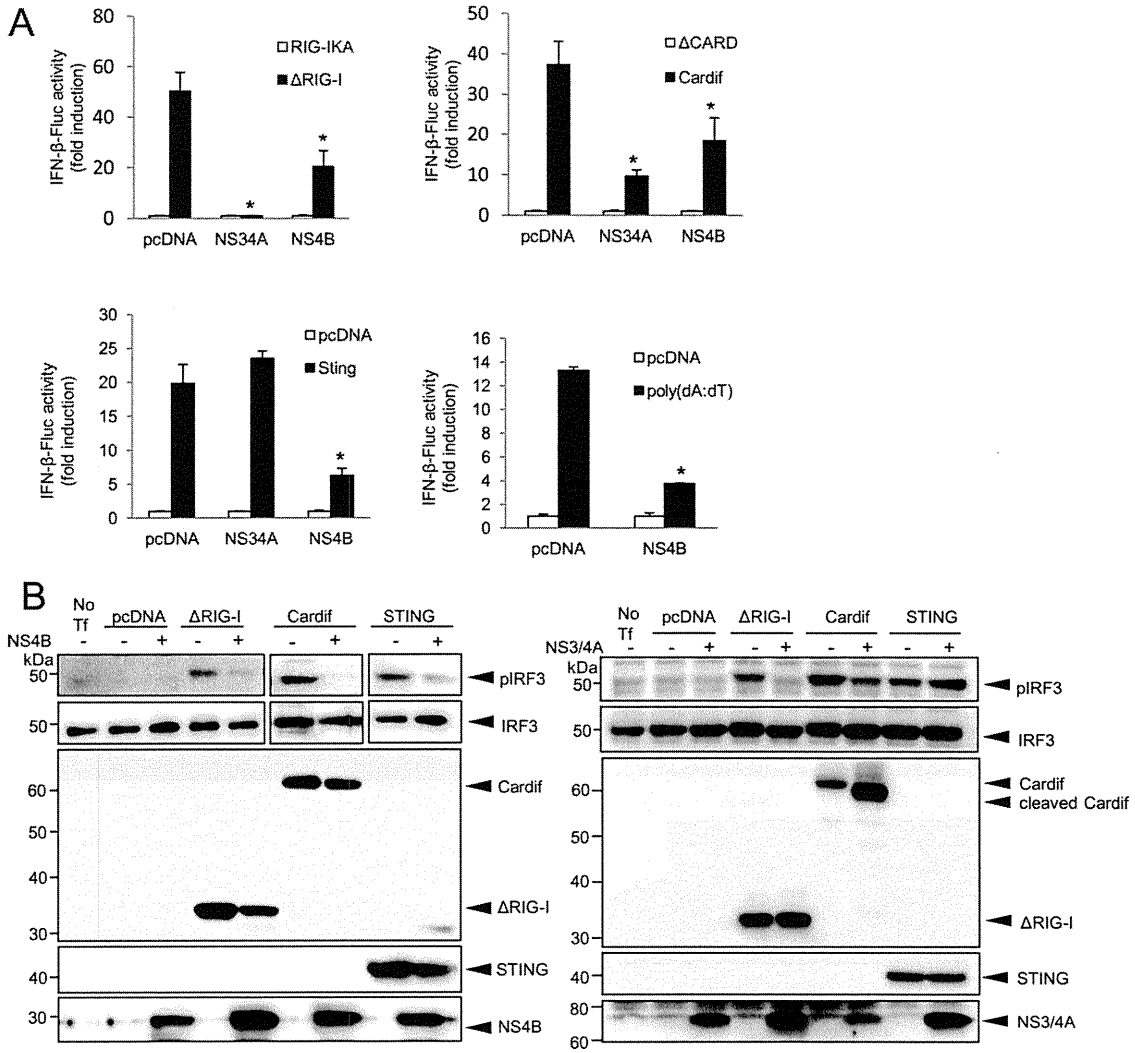


Fig. 1. NS4B suppressed IFN-$\beta$ signaling mediated by RIG-I, Cardif, or STING. (A) Plasmids expressing ΔRIG-I, Cardif, or STING or poly(dA:dT) as well as NS3/4A or NS4B were cotransfected with pIFN-$\beta$-Fluc and pRL-CMV into HEK293T cells. After 24 hours, dual luciferase assays were performed. Plasmids expressing RIG-IKA, ΔCARD, or an empty plasmid (pcDNA) were used as a corresponding negative control. The experiments were performed more than three times and yielded consistent results. The *y* axis indicates relative IFN-$\beta$-Fluc activity. Assays were performed in triplicate and error bars indicate mean ± SD. $*P < 0.05$. (B) HEK293T cells were cotransfected with indicated plasmids. On the day after transfection, the cells were lysed and immunoblot analyses were performed. No Tf, transfection-negative controls. pIRF-3 and IRF-3, phosphorylated and total IRF-3, respectively.

NS4B suppress RIG-I–mediated IFN-$\beta$ production, but they do so by targeting different molecules in the signaling pathway.

***Subcellular Localization of NS4B, Cardif, and STING.*** We next studied the subcellular localization of NS4B following its overexpression and measured the colocalization of NS4B with Cardif and STING in both HEK293T cells and Huh7 cells by indirect immunofluorescence microscopy. NS4B was localized predominantly in the ER, which is consistent with previous reports[33] (Fig. 2A). Cardif was localized in mitochondria but did not colocalize with the ER-resident host protein disulphide-isomerase (PDI). Interestingly, Cardif and NS4B colocalized partly at the boundary of the two proteins, although their original localization was different (Fig. 2A,C). STING was localized predominantly in the ER[20,21] (Fig. 2B,D). STING colocalized partly with Cardif, which is consistent with a previous report by Ishikawa and Barber[20] (Fig. 2B,D). In cells cotransfected with NS4B and STING expression plasmids, NS4B colocalized precisely with STING (Fig. 2B,D). To examine the region of NS4B-STING interaction, we next observed the two proteins by performing staining for them along with mitochondria-associated ER membrane (MAM), which is a physical association with mitochondria[34] and has been reported the site of Cardif-STING association.[24] Both NS4B and STING were adjacent to and partially colocalized

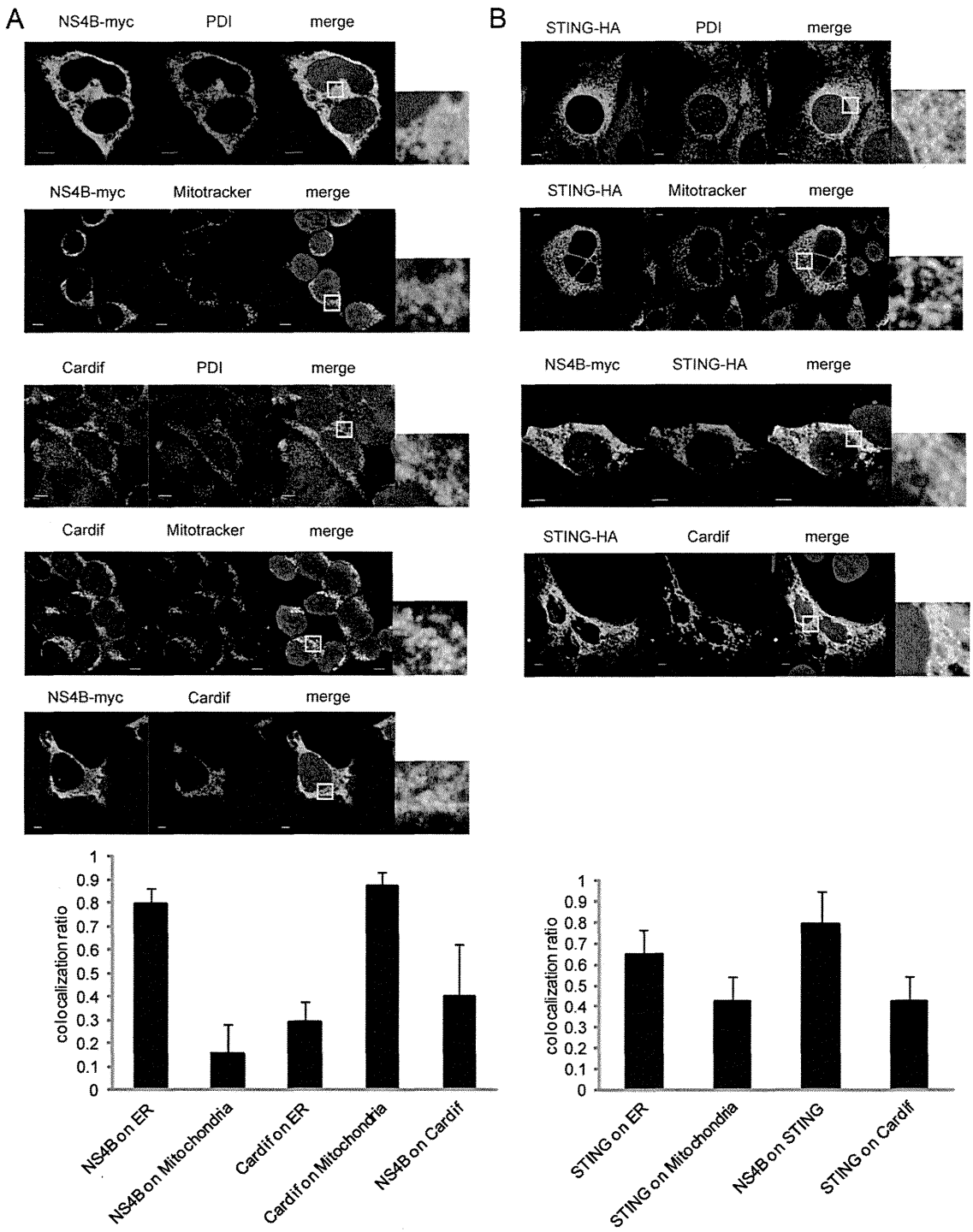


Fig. 2. Subcellular localization of NS4B, Cardif, and STING. (A-D) Subcellular localization of NS4B, Cardif, and STING in 293T (A,C) and Huh7 (B,D) cells. (A,C) NS4B-myc (first, second, and fifth panels of A and third panel of C) was transfected, and 24 hours later the cells were fixed and immunostained with anti-myc. In the third, fourth, and fifth panels of A, and the first and second panels of C, endogenous Cardif was detected with anti-Cardif antibody. ER was immunostained with anti-PDI antibody (first and third panels of A and first panel of C). Mitochondria were stained using Mitotracker (second and fourth panels of A and second panel of C). Nuclei were stained with 4',6-diamidino-2-phenylindole (DAPI). (B,D) STING-HA (all panels) and NS4B-myc (third panels) were transfected, and after 24 hours the cells were fixed and immunostained with anti-HA or anti-myc, respectively. In the fourth panels, endogenous Cardif was detected with anti-Cardif antibody. ER was immunostained with anti-PDI antibody (first panels). Mitochondria were stained using Mitotracker (second panels). Nuclei were stained with DAPI. (E) NS4B-myc and STING-HA were transfected into Huh7 cells and after 24 hours the cells were fixed and immunostained with anti-HA, anti-myc, and anti-FACL4 (MAM) antibody. Cells were visualized by confocal microscopy. Scale bars indicate 5 $\mu$m. In each microscopic image, the grade of protein colocalization in a single cell was quantified and is shown in the graphs at the bottom of each panel. Values are shown as the average colocalization ratio in 8 cells. Error bars indicate the mean + SD.

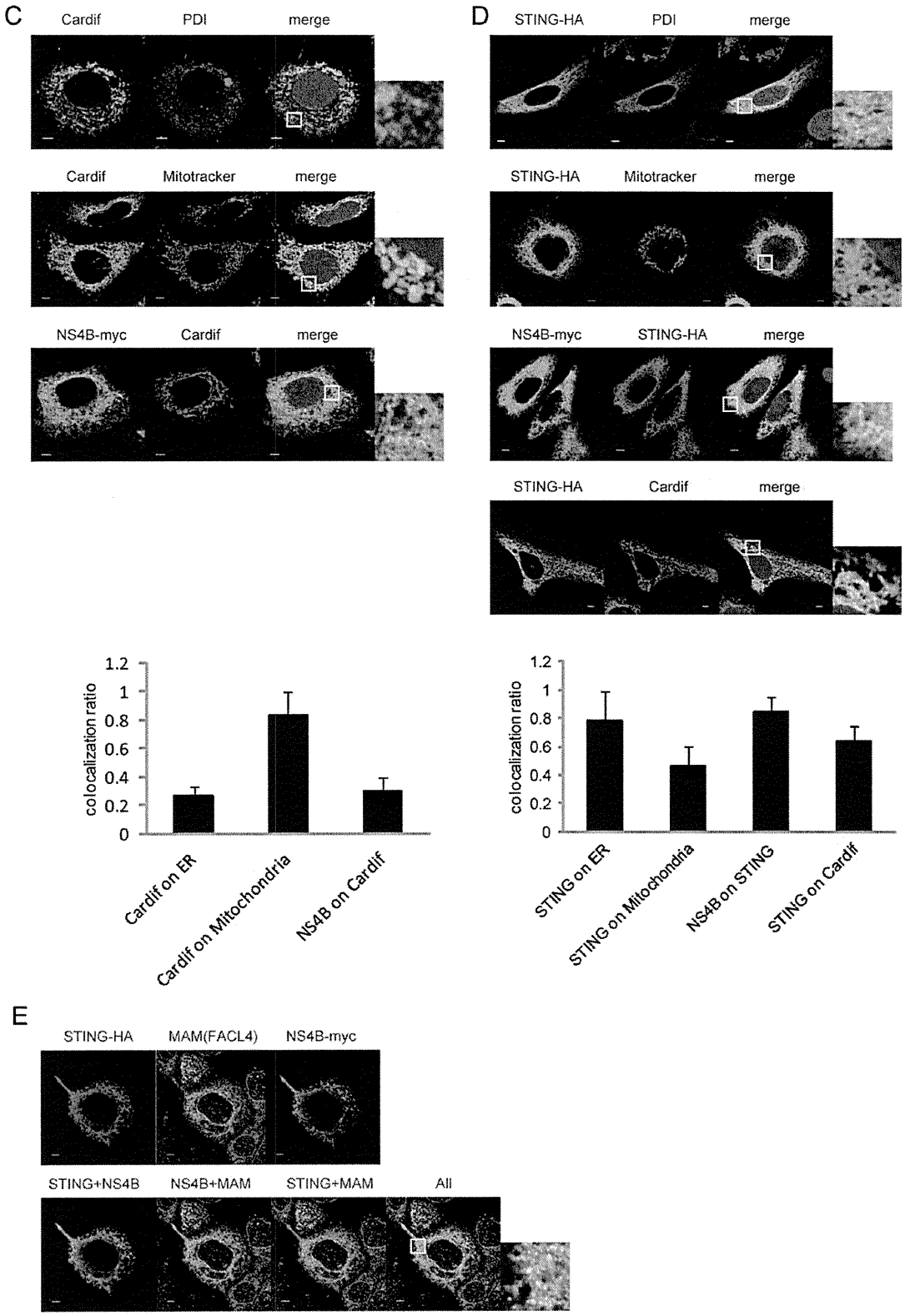


Fig. 2. Continued

with fatty acid-CoA ligase long chain 4 (FACL4), which is a MAM marker protein[35,36] (Fig. 2E). These findings suggest that NS4B might interact with STING on MAM more strongly than with Cardif.

***Protein-Protein Interaction Between NS4B, Cardif, and STING.*** Knowing that NS4B was colocalized strongly with STING and only partly with Cardif, we next analyzed direct protein-protein interactions

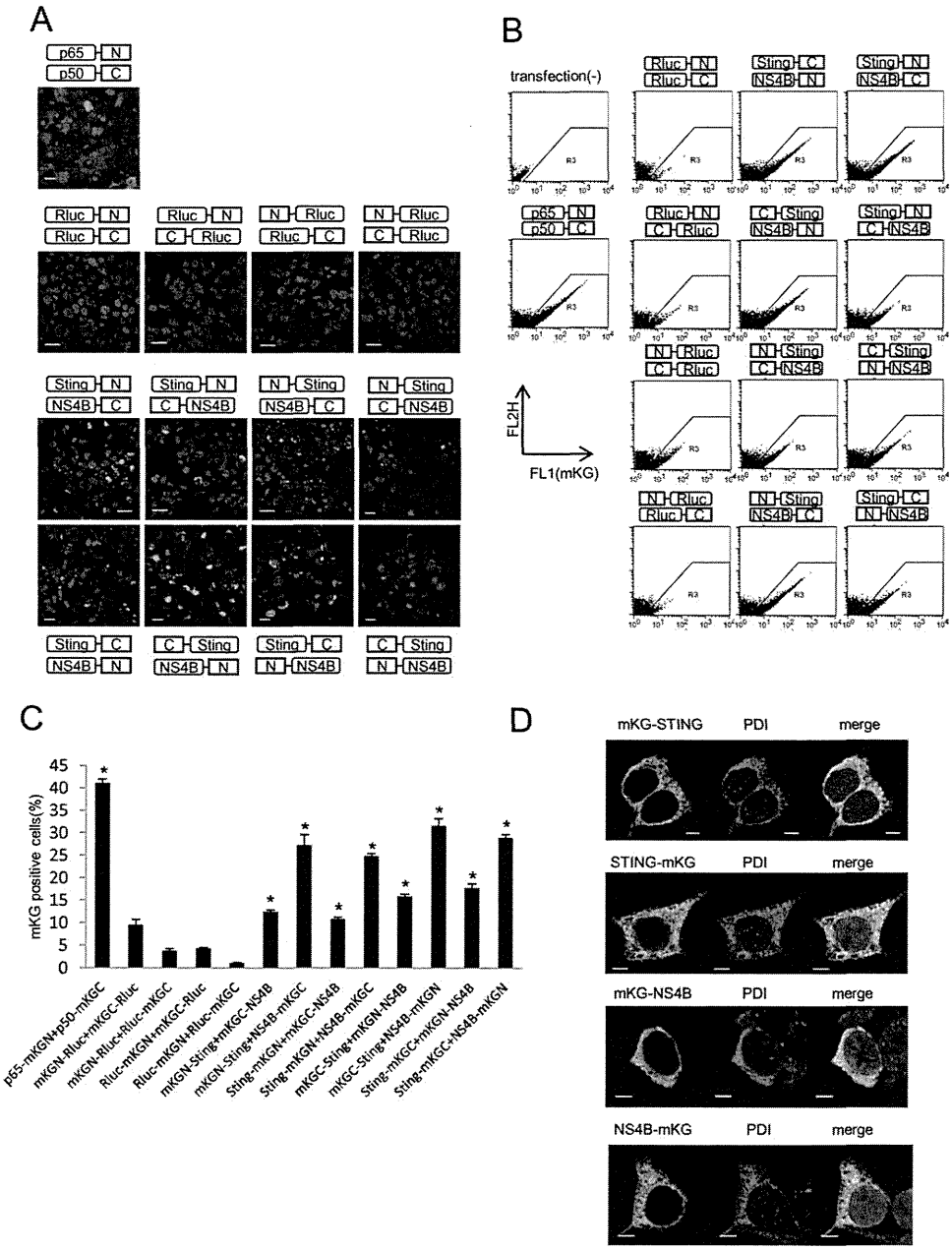


Fig. 3. BiFC assays of STING and NS4B. The complementary pairs of N- or C-terminally mKG-fused NS4B and STING expression plasmids were cotransfected in HEK293T cells. After 24 hours, the cells were fixed and observed by confocal microscopy (A) or subjected to flow cytometry to measure mKG-emitted fluorescence (BiFC signal) and to count BiFC signal-positive cells (B,C). Plasmids expressing p65-mKGN and p50-mKGC individually were used as a BiFC-positive control and plasmids expressing N- or C-terminally mKG fused Rluc were used as a negative control. The letters N and C denote complimentary N- and C-terminal fragments of mKG, respectively. Assays were performed in triplicate and error bars indicate the mean ± SD. Scale bars indicate 10 $\mu$m (A). *$P < 0.05$ compared with corresponding negative controls. (D) Plasmids expressing mKG fragment-fused STING or NS4B were transfected in HEK293T cells. After 24 hours, the cells were fixed and immunostained with anti-mKG and anti-PDI (ER) antibody. Nuclei were stained with DAPI. Cells were observed by confocal microscopy. Scale bars = 5 $\mu$m.

between NS4B, Cardif, and STING. To detect those interactions in living cells, we performed BiFC assays.[37,38] We constructed NS4B, Cardif, and STING expression plasmids that were N- or C-terminally fused with truncated mKG proteins, respectively. First, we cotransfected several different pairs of NS4B and STING expression plasmids that were fused with complementary pairs of N- or C-terminally truncated mKG. Strong fluorescence by mKG complexes (BiFC signal) was detected in all pairs of cotransfections, suggesting significant molecular interaction (Fig. 3A). In flow cytometry, all pairs of NS4B- and STING-mKG fusion proteins were positive for strong BiFC signal (Fig. 3B). The percentages of cells positive for BiFC signal were significantly higher in STING-mKG and NS4B-mKG fusion complexes than in corresponding controls (Fig. 3C). These results demonstrate that HCV-NS4B and STING proteins interact with each other strongly and specifically in cells. Fluorescence microscopy indicated that N- and C-terminal fusion of mKG onto NS4B and STING did not affect subcellular localization (Fig. 3D).

We next studied the molecular interaction between NS4B and Cardif by BiFC assay using NS4B and Cardif fusion plasmids that were tagged with complementary pairs of truncated mKG. Weak fluorescence was detected in cells transfected with the pairs N-Cardif and NS4B-C, N-Cardif and C-NS4B, C-Cardif and

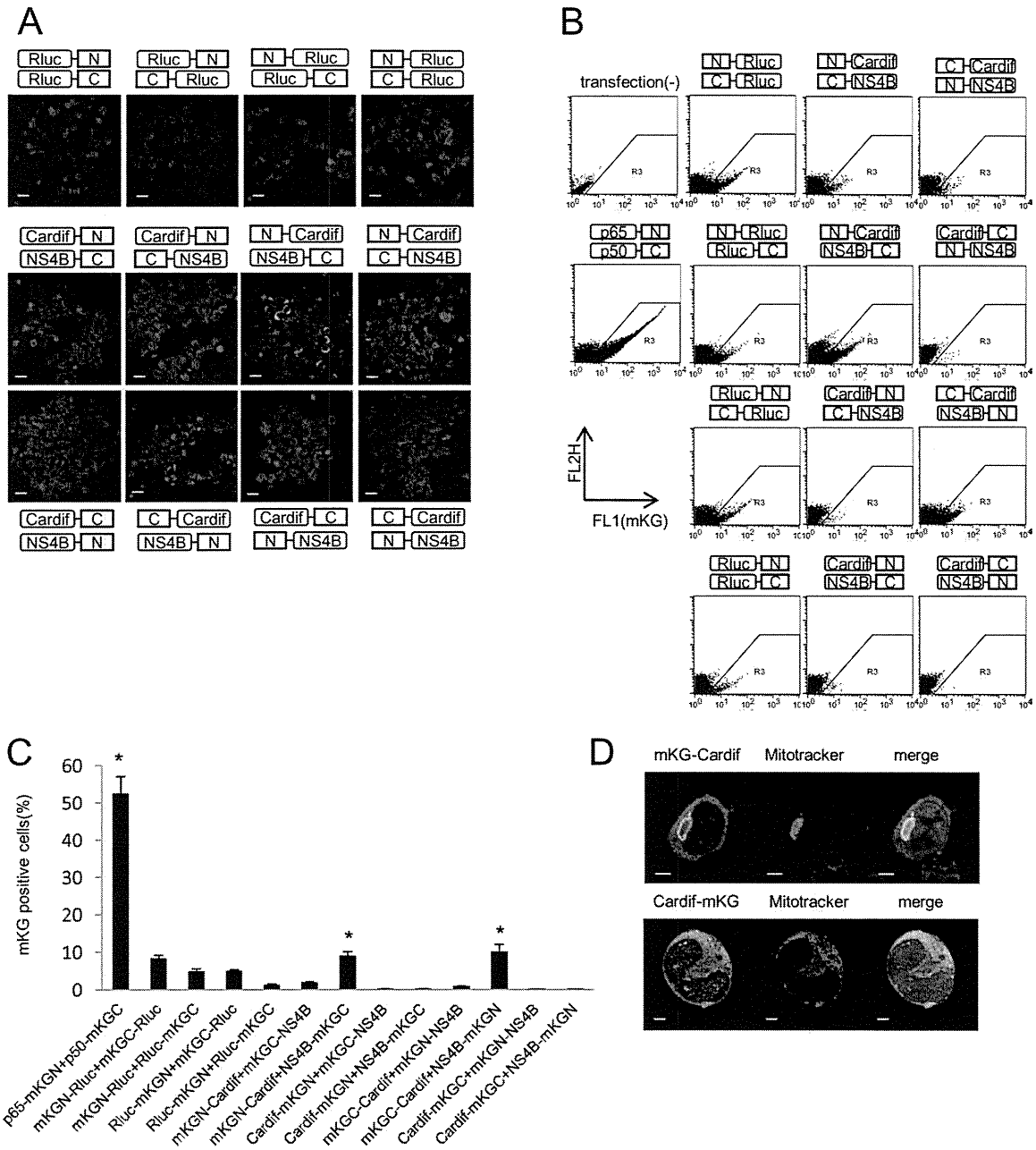


Fig. 4. BiFC assays of Cardif and NS4B. The complementary pairs of N- or C-terminally mKG-fused NS4B and Cardif expression plasmids were cotransfected in HEK293T cells. After 24 hours, the cells were fixed and observed by confocal microscopy (A) or subjected to flow cytometry to measure mKG-emitted fluorescence (BiFC signal) and to count BiFC signal-positive cells (B,C). Plasmids expressing p65-mKGN and p50-mKGC individually were used as a BiFC-positive control and plasmids expressing N- or C-terminally mKG-fused Rluc were used as a negative control. The letters N and C denote complimentary N- and C-terminal fragments of mKG, respectively. Assays were performed in triplicate, and error bars indicate the mean ± SD. Scale bars indicate 10 $\mu$m (A). *$P < 0.05$ compared with corresponding negative controls. (D) Plasmids expressing mKG fragment-fused STING or NS4B were transfected in HEK293T cells. After 24 hours, the cells were fixed and immunostained with anti-mKG antibody. Mitochondria were stained using Mitotracker, and nuclei were stained with DAPI. Cells were observed by confocal microscopy. Scale bars = 5 $\mu$m.

NS4B-N, and C-Cardif and N-NS4B (Fig. 4A,B). The percentage of cells positive for BiFC signal increased with the combination of N-Cardif and NS4B-C, and C-Cardif and NS4B-N (Fig. 4C). Fluorescence microscopy indicated that mKG-Cardif, but not Cardif-mKG, was partially colocalized with mitochondria, possibly due to disruption of mitochondria anchor domain by C-terminal fusion with mKG (Fig. 4D). These results indicate the lack of significant molecular interactions between NS4B and Cardif.

***Binding of NS4B to STING Blocks Molecular Interaction Between Cardif and STING.*** It has been reported that STING binds Cardif directly.[20,22] Thus, we hypothesized that NS4B, through a competitive

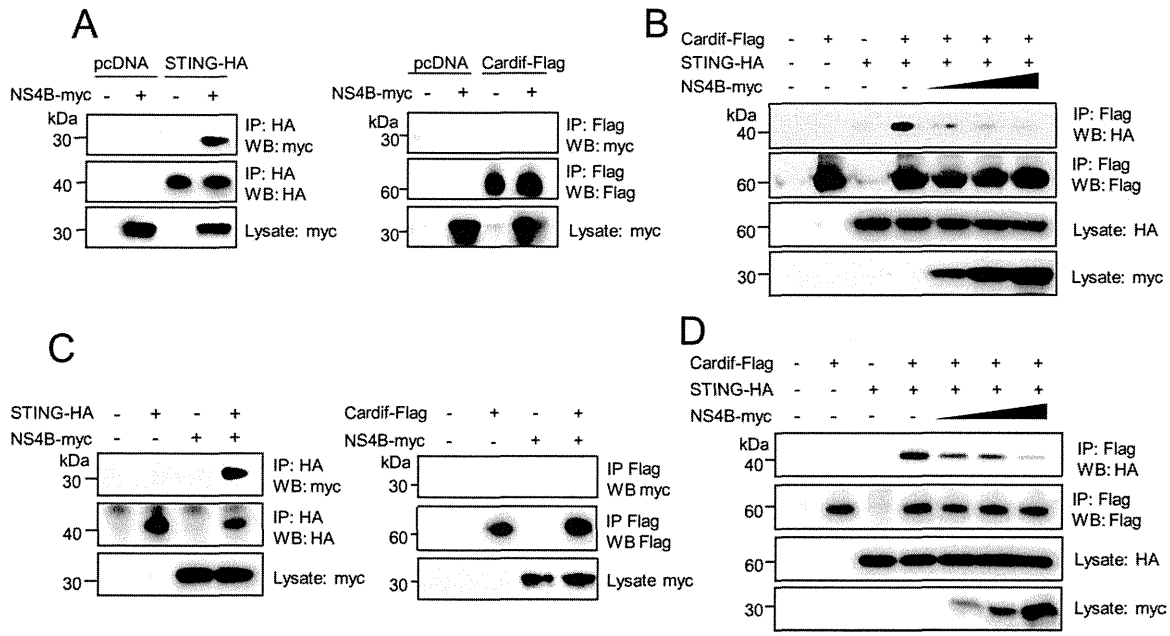


Fig. 5. Binding of NS4B to STING blocks molecular the interaction between Cardif and STING. (A,C) NS4B expression plasmid was cotransfected with STING or Cardif expression plasmid into HEK293T cells (A) or Huh7 cells (C). After 24 hours, cell lysates were subjected to immunoprecipitation using anti-HA or anti-Flag and were immunoblotted with anti-myc. (B,D) Cardif and STING expression plasmids were cotransfected with various amounts of NS4B plasmid in HEK293T cells (B) or Huh7 cells (D). After 24 hours, cells lysates were subjected to immunoprecipitation using anti-Flag and were immunoblotted with anti-HA.

interaction with STING, may hinder the direct molecular interaction between Cardif and STING. To verify this hypothesis, we performed immunoprecipitation assays. First, we transfected plasmids that expressed NS4B and Cardif, or NS4B and STING, in HEK293T cells or Huh7 cells, and performed immunoprecipitation. NS4B strongly bound to STING in both HEK293T cells and Huh7 cells, suggesting specific molecular interactions, whereas NS4B and Cardif did not show any obvious interaction (Fig. 5A,C). Consistent with previous reports, STING and Cardif showed significant interaction (Fig. 5B,D). Interestingly, those interactions were decreased by coexpression of NS4B, depending on its input amount, and finally blocked completely in both HEK293T and Huh7 cells (Fig. 5B,D). Collectively, the results above demonstrate that NS4B disrupts the interaction between Cardif and STING possibly through competitive binding to STING.

***Effects on HCV Infection and Replication Levels by STING Knockdown and NS4B Overexpression.*** We next studied the impact of STING-mediated IFN production and its regulation by NS4B on HCV infection and cellular replication. First, we transfected three STING-targeted siRNAs into Huh7/Feo cells (Fig. 6A). As shown in Fig. 6B, STING knockdown cells conferred significantly higher permissibility to HCV replication. We next transfected HCV-JFH1 RNA into Huh7 cells that were transiently transfected with NS4B. As shown in Fig. 6C, HCV core protein expression was significantly higher in NS4B-overexpressed cells. Furthermore, HCV replication was increased significantly in Huh7/Feo cells overexpressing NS4B (Fig. 6D). Taken together, the results above demonstrate that STING and NS4B may negatively or positively regulate cellular permissiveness to HCV replication.

***The N-terminal Domain of NS4B Is Essential for Suppressing IFN-β Promoter Activity Mediated by RIG-I, Cardif, and STING.*** It has been reported that the N-terminal domain of several forms of flaviviral NS4B shows structural homology with STING.[24] We therefore investigated whether the STING homology domain in NS4B is responsible for suppression of IFN-$\beta$ production. We constructed two truncated NS4B expression plasmids, which covered the N terminus (NS4Bt1-84, amino acids 1 through 84) containing the STING homology domain and the C terminus (NS4Bt85-261, amino acids 85 through 261), respectively (Fig. 7A). Immunoblotting showed that NS4Bt1-84 and NS4Bt85-261 yielded protein bands of ~9 kDa and ~20 kDa, respectively. Aberrant bands in the truncated NS4B may be due to alternative posttranslational processing. HEK293T cells were transfected with ΔRIG-I, Cardif, or STING, and NS3/4A or the truncated NS4B, along with IFN-$\beta$-Fluc plasmid, and a reporter assay was performed. NS4Bt1-84 significantly suppressed RIG-I, Cardif, and STING-

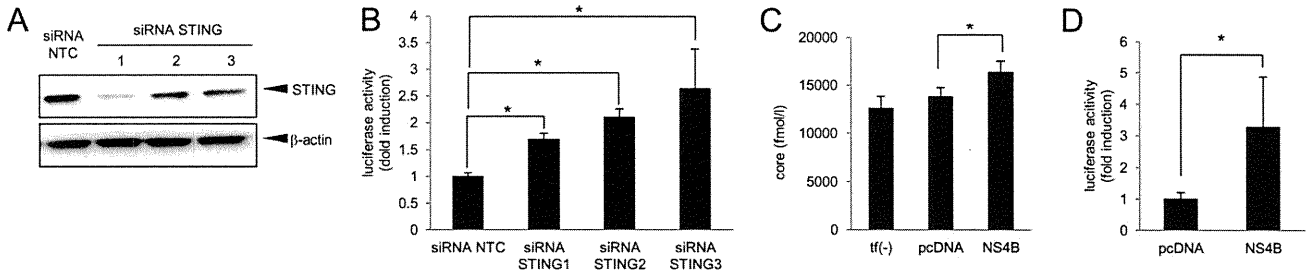


Fig. 6. Effects on HCV replication levels by STING knockdown and NS4B overexpression. (A) Effects of siRNA knockdown of STING by siRNA. Huh7 cells were transfected with STING-targeted siRNAs (siRNA STING-1, -2, and -3, respectively) or negative control siRNA (siRNA NTC). Seventy-two hours after transfection, cells were harvested and expression levels of STING protein were detected by immunoblotting. (B) Huh7 cells expressing HCV-Feo subgenomic replicon (Huh7/Feo)[27,28] were transfected with STING-targeted siRNAs or negative control siRNA. Seventy-two hours after transfection, cells were harvested, and internal luciferase activities were measured. The *y* axis indicates luciferase activity shown as a ratio of transfection-negative control. Assays were performed in triplicate, and error bars indicate the mean + SD. $*P < 0.05$ compared with corresponding negative controls. (C) Empty plasmid or plasmid expressing NS4B was transfected into Huh7 cells. After 24 hours, HCV-JFH1 RNA was transfected into these cells. Seventy-two hours after virus transfection, HCV core antigen levels in culture medium were measured. Assays were performed in triplicate, and error bars indicate the mean + SD. $*P < 0.05$ compared with corresponding negative controls. tf(−), transfection-negative control. (D) Huh7 cells expressing HCV-Feo replicon (Huh7/Feo)[27,28] were transfected with NS4B expressing plasmid or empty plasmid (pcDNA). Forty-eight hours after transfection, internal luciferase activities were measured. The *y* axis indicates luciferase activity shown as a ratio of the transfection-negative control. Assays were performed in triplicate, and error bars indicate the mean + SD. $*P < 0.05$ compared with corresponding negative controls.

induced IFN-$\beta$ promoter activity, whereas NS4Bt85-261 did not (Fig. 7B). These results suggest that the N-terminal domain of NS4B is responsible for association with STING. Fluorescent microscopy indicated that both NS4Bt1-84 and NS4Bt85-26 colocalized with ER and STING (Fig. 7C).

***NS4B Suppresses IFN Production Signaling Cooperatively with NS3/4A.*** It has been reported that

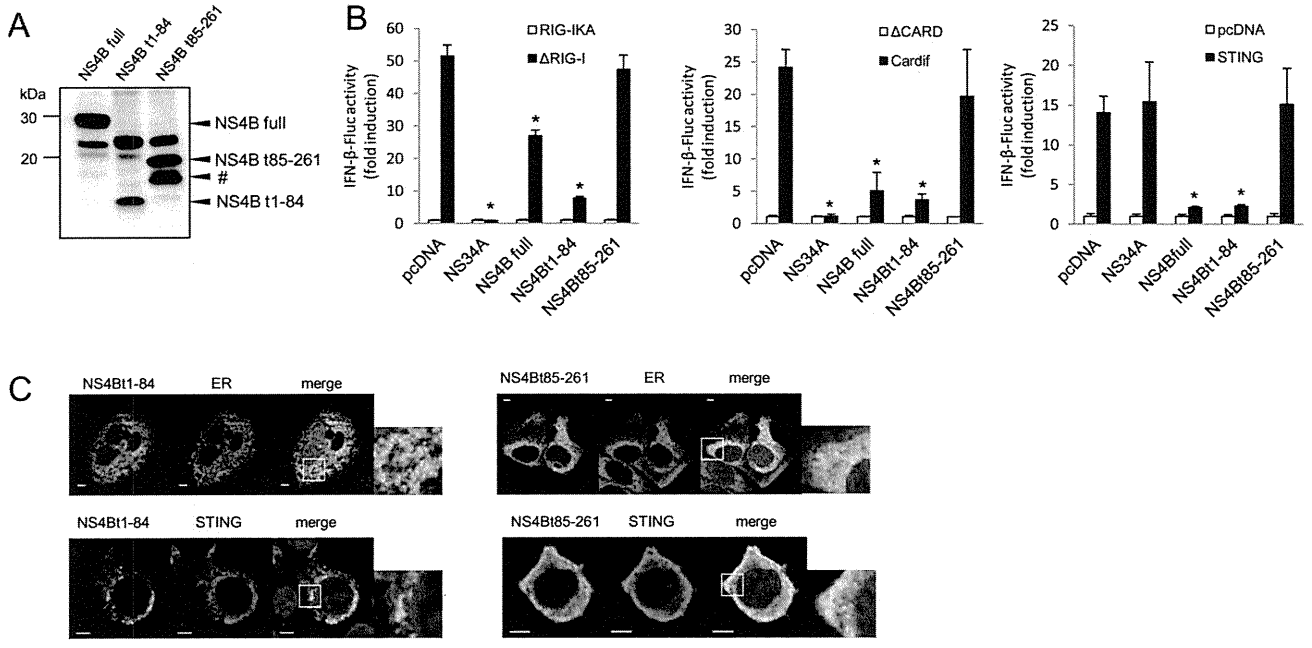


Fig. 7. The N-terminal domain of NS4B is essential for suppressing IFN-$\beta$ promoter activity induced by RIG-I, Cardif, or STING. (A) Immunoblotting of NS4B and truncated NS4B, NS4B t1-84, and NS4Bt85-216. HEK293T cells were transfected with NS4B or truncated NS4B. After 24 hours, the cells were lysed and immunoblot assays were performed. The band indicated by the pound sign (#) is a truncated NS4B, probably generated via alternative posttranslational processing. (B) Plasmids expressing ΔRIG-I, Cardif, or STING as well as NS3/4A or the indicated truncated form of NS4B were cotransfected with pIFN-$\beta$-Fluc and pRL-CMV in HEK293T cells. Dual luciferase assays were performed 24 hours after transfection. Plasmids expressing RIG-IKA, ΔCARD, or pcDNA were used as negative controls. The *y* axis indicates IFN-$\beta$-Fluc activity shown as relative values. Assays were performed in triplicate, and error bars indicate the mean ± SD. $*P < 0.05$ compared with corresponding negative controls. (C) Plasmids expressing NS4Bt1-84-myc of NS4Bt85-261-myc were transfected with or without plasmids expressing HA-STING in HEK293T cells. After 24 hours, the cells were fixed and immunostained. Nuclei were stained with DAPI. Cells were observed by confocal microscopy. Scale bars indicate 5 $\mu$m.

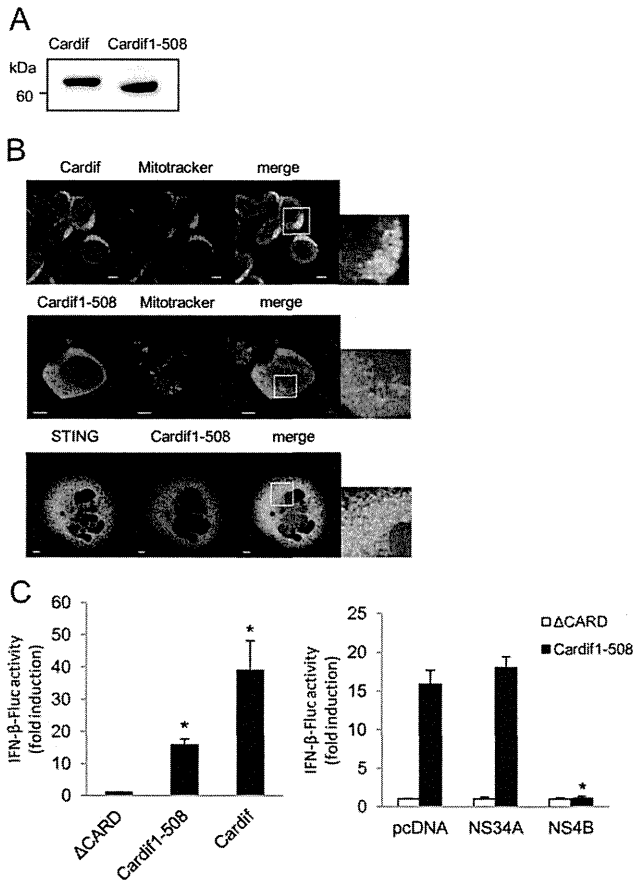


Fig. 8. NS4B suppressed IFN-$\beta$ production pathway independently of and cooperatively with NS3/4A. (A) Immunoblotting of Cardif and truncated Cardif (Cardif1-508). HEK293T cells were transfected with Cardif or truncated Cardif (Cardif1-508). After 24 hours, the cells were lysed and immunoblot assays were performed. (B) Subcellular localization of Cardif and truncated Cardif (Cardif1-508). HEK293T cells were immunostained with anti-Cardif antibody or HEK293T cells were transfected with myc-tagged truncated Cardif (Cardif1-508-myc), and after 24 hours the cells were immunostained with anti-myc. Mitochondria were stained with Mitotracker (red) and nuclei were stained with DAPI (blue). Plasmid expressing myc-tagged truncated Cardif (Cardif1-508) and plasmid expressing HA-tagged STING were transfected into HEK293T cells. The cells were immunostained with anti-myc and anti-HA antibodies and analyzed by confocal laser microscopy. Scale bars = 10 $\mu$m. (C) Plasmids expressing Cardif or truncated Cardif (Cardif1-508) and pIFN-$\beta$-Fluc and pRL-CMV were transfected with or without plasmid expressing NS3/4A or NS4B into HEK293T cells as indicated. Dual luciferase assays were performed 24 hours after transfection. Plasmid expressing ΔCARD or pcDNA was used as a negative control. The *y* axis indicates IFN-$\beta$-Fluc activity shown as relative values. Assays were performed in triplicate, and error bars indicate the mean ± SD. $^*P < 0.05$.

HCV NS3/4A serine protease cleaves Cardif between Cys-508 and His-509, releases Cardif from the mitochondrial membrane, and blocks RIG-I–induced IFN-$\beta$ production. We next assessed whether NS4B suppresses IFN-$\beta$ production in the presence of Cardif cleaved by NS3/4A protease (Cardif1-508, Fig. 8A). The truncation of Cardif–C-terminal residue abolished mitochondrial localization but still colocalized with STING (Fig. 8B). The reporter assay showed that Cardif1-508 induced weak IFN-$\beta$ activation. Interestingly, NS4B completely blocked the residual function of the Cardif1-508 protein to activate IFN-$\beta$ expression, suggesting an additive effect of NS3/4A and NS4B on the RIG-I–activating pathway (Fig. 8C).

## Discussion

It has been reported that viruses, including HCV, target IFN signaling to establish persistent replication in host cells.[39] We have reported that NS4B blocks the transcriptional activation of ISRE induced by overexpression of RIG-I and Cardif, but not by TBK1 or IKK$\epsilon$.[19] In the present study, we have shown that NS4B directly and specifically binds STING, an ER-residing scaffolding protein of Cardif and TBK1 and an inducer of IFN-$\beta$ production (Figs. 3 and 5), and blocked the interaction between STING and Cardif (Fig. 5B,D) resulting in strong suppression of RIG-I–mediated phosphorylation of IRF-3 and expressional induction of IFN-$\beta$ (Fig. 1). Furthermore, HCV replication was increased by knockdown of STING or overexpression of NS4B (Fig. 6). Taken together, our results demonstrate that HCV-NS4B strongly blocks virus-induced, RIG-I–mediated activation of IFN-$\beta$ production signaling through targeting STING, which constitutes a novel mechanism of viral evasion from innate immune responses and establishment of persistent viral replication.

Our results also showed that the effects of NS4B on the RIG-I signaling were independent of NS3/4A-mediated cleavage of Cardif. Reporter assays showed that a cleaved form of Cardif (Cardif1-508) partially retained activity for the induction of IFN-$\beta$ promoter activation. The residual IFN-$\beta$ promoter activation was suppressed almost completely by NS4B but not by NS3/4A (Fig. 8C). These findings show that there are at least two mechanisms by which HCV can abrogate RIG-I–mediated IFN production signaling to accomplish abrogation of cellular antiviral responses.

NS4B and STING are ER proteins,[20,21,40] whereas Cardif is localized on the outer mitochondrial membrane.[9] Consistent with those reports, our immunostaining experiments demonstrated that most NS4B protein colocalized with STING (Fig. 2), and their association was localized on MAM (Fig. 2E). In addition to the significant colocalization of STING and NS4B, STING partially colocalized with Cardif at the boundary region of the two proteins (Fig. 2B). Furthermore, immunoprecipitation experiments showed that overexpression of NS4B completely blocked the interaction of STING with Cardif (Fig. 5B). Ishikawa et al.[24] reported

that STING could associate with Cardif by MAM interaction. Castanier et al.[41] reported that Cardif-STING interaction was enhanced in cells with elongated mitochondria. In addition, Horner et al.[42,43] observed NS3/4A targeting of MAM-anchored synapse and cleavage of Cardif at MAM but not in mitochondria. These results led us to speculate that interaction between STING and Cardif was enhanced by altering their subcellular localization during viral infection and that NS4B inhibits Cardif activation by interfering with the association between STING and Cardif on MAM-like NS3/4A behavior against host innate immunity.

HCV-NS4B is an ER-localized 27-kDa protein with several functions in the HCV life cycle. Cellular expression of NS4B induces convolution of the ER membrane and formation of a membranous web that harbors HCV replicase complex.[44,45] NS4B also has RNA-binding capacity.[46] In addition, several point mutations of NS4B were found to alter viral replication activity.[33,46,47] The studies above indicate that NS4B provides an important protein-protein or protein-RNA interaction platform within the HCV replication complex and is essential for viral RNA replication. However, there are few reports on the involvement of NS4B with antiviral immune responses. Consistent with our previous study, Moriyama et al.[48] reported that NS4B partially inhibited dsRNA-induced but not TRIF-induced activation of IFN-$\beta$. In NS4B-expressing cells, IFN-$\alpha$ induced activation of STAT1 was suppressed.[49] The present study has demonstrated that NS4B functions against the host IFN response, such that NS4B directly interacts with STING and suppresses downstream signaling, resulting in the induction of IFN production.

STING contains a domain homologous to the N terminus of NS4B derived from several flaviviruses, including HCV. In our previous NS4B truncation assay, the NS4B N-terminal domain (amino acids 1-110) was important for suppression of RIG-I–induced IFN-$\beta$ expression.[19] Consistent with these results, N-terminally truncated NS4B (NS4Bt1-84) significantly suppressed STING and Cardif-induced IFN-$\beta$ promoter activation, whereas the C terminus of NS4B (NS4Bt85-261) did not (Fig. 7). These results reinforce our hypothesis that NS4B binds STING at its homology domain and blocks the ability of STING to induce IFN-$\beta$ production.

A small molecule inhibitor of NS4B has been developed and is under preliminary clinical trials.[50] Einav et al.[51] identified clemizole hydrochloride, an H1 histamine receptor antagonist, as an inhibitor of the RNA-binding function of NS4B and HCV RNA replication. A phase 1B clinical trial of clemizole in hepatitis C patients has been completed.[52] Other two NS4B inhibitors which are a compound of amiloride analog and anguizole are under preclinical development.[53,54] The possibility remains that such NS4B inhibitors may suppress HCV replication partly through inhibiting the ability of NS4B to suppress IFN-$\beta$ production and restore cellular antiviral responses.

In conclusion, IFN production signaling induced by HCV infection and mediated by RIG-I is suppressed by NS4B through a direct interaction with STING. These virus-host interactions help to elucidate the mechanisms of persistent HCV infection and constitute a potential target to block HCV infection.

*Acknowledgment:* The authors are indebted to J. Tcshopp for providing Cardif, ΔCARD, and CARD and to G. N. Barber for the STING plasmids. This study was supported by grants from the Ministry of Education, Culture, Sports, Science and Technology, Japan; the Japan Society for the Promotion of Science; Ministry of Health, Labour and Welfare, Japan; and the Japan Health Sciences Foundation.

## References

1. Samuel CE. Antiviral actions of interferons. Clin Microbiol Rev 2001; 14:778-809.
2. Taniguchi T, Takaoka A. The interferon-alpha/beta system in antiviral responses: a multimodal machinery of gene regulation by the IRF family of transcription factors. Curr Opin Immunol 2002;14:111-116.
3. Sakamoto N, Watanabe M. New therapeutic approaches to hepatitis C virus. J Gastroenterol 2009;44:643-649.
4. Bigger CB, Brasky KM, Lanford RE. DNA microarray analysis of chimpanzee liver during acute resolving hepatitis C virus infection. J Virol 2001;75:7059-7066.
5. Yoneyama M, Kikuchi M, Natsukawa T, Shinobu N, Imaizumi T, Miyagishi M, et al. The RNA helicase RIG-I has an essential function in duoble-stranded RNA-induced innate antiviral responses. Nat Immunol 2004;5:730-737.
6. Hornung V, Ellegast J, Kim S, Brzozka K, Jung A, Kato H, et al. 5'-Triphosphate RNA is the ligand for RIG-I. Science 2006;314:994-997.
7. Takahasi K, Yoneyama M, Nishihori T, Hirai R, Kumeta H, Narita R, et al. Nonself RNA-sensing mechanism of RIG-I helicase and activation of antiviral immune responses. Mol Cell 2008;29:428-440.
8. Kawai T. IPS-1, an adaptor triggering RIG-I- and Mda5-mediated type I interferon induction. Nat Immunol 2005;6:981-988.
9. Seth RB, Sun L, Ea CK, Chen ZJ. Identification and characterization of MAVS, a mitochondrial antiviral signaling protein that activates NF-κB and IRF 3. Cell 2005;122:669-682.
10. Xu LG. VISA is an adapter protein required for virus-triggered IFN-β signaling. Mol Cell 2005;19:727-740.
11. Meylan E, Curran J, Hofmann K, Moradpour D, Binder M, Bartenschlager R, et al. Cardif is an adaptor protein in the RIG-I antiviral pathway and is targeted by hepatitis C virus. Nature 2005;437: 1167-1172.
12. Yoneyama M, Suhara W, Fukuhara Y, Fukuda M, Nishida E, Fujita T. Direct triggering of the type I interferon system by virus infection: activation of a transcription factor complex containing IRF-3 and CBP/p300. EMBO J 1998;17:1087-1095.

13. Lin W, Kim SS, Yeung E, Kamegaya Y, Blackard JT, Kim KA, et al. Hepatitis C virus core protein blocks interferon signaling by interaction with the STAT1 SH2 domain. J Virol 2006;80:9226-9235.
14. Suda G, Sakamoto N, Itsui Y, Nakagawa M, Tasaka-Fujita M, Funaoka Y, et al. IL-6-mediated intersubgenotypic variation of interferon sensitivity in hepatitis C virus genotype 2a/2b chimeric clones. Virology 2010;407:80-90.
15. Funaoka Y, Sakamoto N, Suda G, Itsui Y, Nakagawa M, Kakinuma S, et al. Analysis of interferon signaling by infectious hepatitis C virus clones with substitutions of core amino acids 70 and 91. J Virol 2011; 85:5986-5994.
16. Loo YM, Owen DM, Li K, Erickson AK, Johnson CL, Fish PM, et al. Viral and therapeutic control of IFN-beta promoter stimulator 1 during hepatitis C virus infection. Proc Natl Acad Sci U S A 2006;103:6001-6006.
17. Li X-D, Sun L, Seth RB, Pineda G, Chen ZJ. Hepatitis C virus protease NS3/4A cleaves mitochondrial antiviral signaling protein off the mitochondria to evade innate immunity. Proc Natl Acad Sci U S A 2005; 102:17717-17722.
18. Baril M, Racine M-E, Penin F, Lamarre D. MAVS Dimer Is a Crucial Signaling Component of Innate Immunity and the Target of Hepatitis C Virus NS3/4A Protease. J. Virol. 2009;83:1299-1311.
19. Tasaka M, Sakamoto N, Itakura Y, Nakagawa M, Itsui Y, Sekine-Osajima Y, et al. Hepatitis C virus non-structural proteins responsible for suppression of the RIG-I/Cardif-induced interferon response. J Gen Virol 2007;88:3323-3333.
20. Ishikawa H, Barber GN. STING is an endoplasmic reticulum adaptor that facilitates innate immune signalling. Nature 2008;455:674-678.
21. Sun W, Li Y, Chen L, Chen H, You F, Zhou X, et al. ERIS, an endoplasmic reticulum IFN stimulator, activates innate immune signaling through dimerization. Proc Natl Acad Sci U S A 2009;106:8653-8658.
22. Zhong B, Yang Y, Li S, Wang YY, Li Y, Diao F, et al. The adaptor protein MITA links virus-sensing receptors to IRF3 transcription factor activation. Immunity 2008;29:538-550.
23. Jin L. MPYS, a novel membrane tetraspanner, is associated with major histocompatibility complex class II and mediates transduction of apoptotic signals. Mol Cell Biol 2008;28:5014-5026.
24. Ishikawa H, Ma Z, Barber GN. STING regulates intracellular DNA-mediated, type I interferon-dependent innate immunity. Nature 2009; 461:788-792.
25. Yanagi M, Purcell RH, Emerson SU, Bukh J. Transcripts from a single full-length cDNA clone of hepatitis C virus are infectious when directly trasfected into the liver of a chimpanzee. Proc Natl Acad Sci U S A 1997;94:8738-8743.
26. Lin R, Lacoste J, Nakhaei P, Sun Q, Yang L, Paz S, et al. Dissociation of a MAVS/IPS-1/VISA/Cardif-IKKepsilon molecular complex from the mitochondrial outer membrane by hepatitis C virus NS3-4A proteolytic cleavage. J Virol 2006;80:6072-6083.
27. Yokota T, Sakamoto N, Enomoto N, Tanabe Y, Miyagishi M, Maekawa S, et al. Inhibition of intracellular hepatitis C virus replication by synthetic and vector-derived small interfering RNAs. EMBO Rep 2003;4:602-608.
28. Tanabe Y, Sakamoto N, Enomoto N, Kurosaki M, Ueda E, Maekawa S, et al. Synergistic inhibition of intracellular hepatitis C virus replication by combination of ribavirin and interferon- alpha. J Infect Dis 2004;189:1129-1139.
29. Wakita T, Pietschmann T, Kato T, Date T, Miyamoto M, Zhao Z, et al. Production of infectious hepatitis C virus in tissue culture from a cloned viral genome. Nat Med 2005;11:791-796.
30. Lindenbach BD, Evans MJ, Syder AJ, Wolk B, Tellinghuisen TL, Liu CC, et al. Complete replication of hepatitis C virus in cell culture. Science 2005;309:623-626.
31. Nakagawa M, Sakamoto N, Enomoto N, Tanabe Y, Kanazawa N, Koyama T, et al. Specific inhibition of hepatitis C virus replication by cyclosporin A. Biochem Biophys Res Commun 2004;313:42-47.
32. Yamashiro T, Sakamoto N, Kurosaki M, Kanazawa N, Tanabe Y, Nakagawa M, et al. Negative regulation of intracellular hepatitis C virus replication by interferon regulatory factor 3. J Gastroenterol 2006;41:750-757.
33. Lindstrom H, Lundin M, Haggstrom S, Persson MA. Mutations of the hepatitis C virus protein NS4B on either side of the ER membrane affect the efficiency of subgenomic replicons. Virus Res 2006;121: 169-178.
34. Hayashi T, Rizzuto R, Hajnoczky G, Su TP. MAM: more than just a housekeeper. Trends Cell Biol 2009;19:81-88.
35. Lewin TM, Van Horn CG, Krisans SK, Coleman RA. Rat liver acyl-CoA synthetase 4 is a peripheral-membrane protein located in two distinct subcellular organelles, peroxisomes, and mitochondrial-associated membrane. Arch Biochem Biophys 2002;404:263-270.
36. Simmen T, Aslan JE, Blagoveshchenskaya AD, Thomas L, Wan L, Xiang Y, et al. PACS-2 controls endoplasmic reticulum-mitochondria communication and Bid-mediated apoptosis. EMBO J 2005;24:717-729.
37. Kerppola TK. Design and implementation of bimolecular fluorescence complementation (BiFC) assays for the visualization of protein interactions in living cells. Nat Protoc 2006;1:1278-1286.
38. Kerppola TK. Bimolecular fluorescence complementation (BiFC) analysis as a probe of protein interactions in living cells. Annu Rev Biophys 2008;37:465-487.
39. Kato H. Differential roles of MDA5 and RIG-I helicases in the recognition of RNA viruses. Nature 2006;441:101-105.
40. Saitoh T, Fujita N, Hayashi T, Takahara K, Satoh T, Lee H, et al. Atg9a controls dsDNA-driven dynamic translocation of STING and the innate immune response. Proc Natl Acad Sci U S A 2009;106: 20842-20846.
41. Castanier C, Garcin D, Vazquez A, Arnoult D. Mitochondrial dynamics regulate the RIG-I-like receptor antiviral pathway. EMBO Rep 2009;11:133-138.
42. Horner SM, Liu HM, Park HS, Briley J, Gale M. Mitochondrial-associated endoplasmic reticulum membranes (MAM) form innate immune synapses and are targeted by hepatitis C virus. Proc Natl Acad Sci U S A 2011;108:14590-14595.
43. Horner SM, Park HS, Gale M Jr. Control of innate immune signaling and membrane targeting by the hepatitis C virus NS3/4A protease are governed by the NS3 helix α0. J Virol 2012;86:3112-3120.
44. Egger D, Wolk B, Gosert R, Bianchi L, Blum HE, Moradpour D, et al. Expression of Hepatitis C virus proteins induces distinct membrane alterations including a candidate viral replication complex. J Virol 2002;76:5974-5984.
45. Gretton SN, Taylor AI, McLauchlan J. Mobility of the hepatitis C virus NS4B protein on the endoplasmic reticulum membrane and membrane-associated foci. J Gen Virol 2005;86:1415-1421.
46. Einav S, Elazar M, Danieli T, Glenn JS. A nucleotide binding motif in hepatitis C virus (HCV) NS4B mediates HCV RNA replication. J Virol 2004;78:11288-11295.
47. Elazar M, Liu P, Rice CM, Glenn JS. An N-terminal amphipathic helix in hepatitis C virus (HCV) NS4B mediates membrane association, correct localization of replication complex proteins, and HCV RNA replication. J Virol 2004;78:11393-11400.
48. Moriyama M, Kato N, Otsuka M, Shao RX, Taniguchi H, Kawabe T, et al. Interferon-beta is activated by hepatitis C virus NS5B and inhibited by NS4A, NS4B, and NS5A. Hepatol Int 2007;1:302-310.
49. Xu J, Liu S, Xu Y, Tien P, Gao G. Identification of the nonstructural protein 4B of hepatitis C virus as a factor that inhibits the antiviral activity of interferon-alpha. Virus Res 2009;141:55-62.
50. Hofmann WP, Zeuzem S. A new standard of care for the treatment of chronic HCV infection. Nat Rev Gastroenterol Hepatol 2011;8: 257-264.
51. Einav S, Gerber D, Bryson PD, Sklan EH, Elazar M, Maerkl SJ, et al. Discovery of a hepatitis C target and its pharmacological inhibitors by microfluidic affinity analysis. Nat Biotech 2008;26:1019-1027.
52. Rai R, Deval J. New opportunities in anti-hepatitis C virus drug discovery: targeting NS4B. Antiviral Res 2011;90:93-101.
53. Cho NJ, Dvory-Sobol H, Lee C, Cho SJ, Bryson P, Masek M, et al. Identification of a class of HCV inhibitors directed against the nonstructural protein NS4B. Sci Transl Med 2010;2:15ra16.
54. Bryson PD, Cho NJ, Einav S, Lee C, Tai V, Bechtel J, et al. A small molecule inhibits HCV replication and alters NS4B's subcellular distribution. Antiviral Res 2010;87:1-8.

HEPATOLOGY
Official Journal of the American Association for the Study of Liver Diseases

# Wnt5a Signaling Mediates Biliary Differentiation of Fetal Hepatic Stem/Progenitor Cells in Mice

Kei Kiyohashi,[1]* Sei Kakinuma,[1,2]* Akihide Kamiya,[3,7] Naoya Sakamoto,[1,4] Sayuri Nitta,[1] Hideto Yamanaka,[1] Kouhei Yoshino,[1] Junko Fujiki,[1] Miyako Murakawa,[1] Akiko Kusano-Kitazume,[1] Hiromichi Shimizu,[1] Ryuichi Okamoto,[1] Seishin Azuma,[1] Mina Nakagawa,[1] Yasuhiro Asahina,[1,2] Naoki Tanimizu,[5] Akira Kikuchi,[6] Hiromitsu Nakauchi,[3] and Mamoru Watanabe[1]

**The molecular mechanisms regulating differentiation of fetal hepatic stem/progenitor cells, called hepatoblasts, which play pivotal roles in liver development, remain obscure. Wnt signaling pathways regulate the development and differentiation of stem cells in various organs. Although a β-catenin–independent noncanonical Wnt pathway is essential for cell adhesion and polarity, the physiological functions of noncanonical Wnt pathways in liver development are unknown. Here we describe a functional role for Wnt5a, a noncanonical Wnt ligand, in the differentiation of mouse hepatoblasts. Wnt5a was expressed in mesenchymal cells and other cells of wild-type (WT) midgestational fetal liver. We analyzed fetal liver phenotypes in Wnt5a-deficient mice using a combination of histological and molecular techniques. Expression levels of Sox9 and the number of hepatocyte nuclear factor (HNF)1$\beta^+$HNF4$\alpha^-$ biliary precursor cells were significantly higher in Wnt5a-deficient liver relative to WT liver. In Wnt5a-deficient fetal liver, *in vivo* formation of primitive bile ductal structures was significantly enhanced relative to WT littermates. We also investigated the function of Wnt5a protein and downstream signaling molecules using a three-dimensional culture system that included primary hepatoblasts or a hepatic progenitor cell line. *In vitro* differentiation assays showed that Wnt5a retarded the formation of bile duct–like structures in hepatoblasts, leading instead to hepatic maturation of such cells. Whereas Wnt5a signaling increased steady-state levels of phosphorylated calcium/calmodulin-dependent protein kinase II (CaMKII) in fetal liver, inhibition of CaMKII activity resulted in the formation of significantly more and larger-sized bile duct–like structures *in vitro* compared with those in vehicle-supplemented controls. *Conclusion:* Wnt5a-mediated signaling in fetal hepatic stem/progenitor cells suppresses biliary differentiation. These findings also suggest that activation of CaMKII by Wnt5a signaling suppresses biliary differentiation. (HEPATOLOGY 2013;57:2502-2513)**

Hepatic stem cells are multipotent stem cells located within ductal plates in fetal and neonatal livers, and canals of Hering in pediatric and adult livers.[1] The extrahepatic stem cell niches are peribiliary glands within the bile ducts in humans.[2] Hepatic stem/progenitor cells, called hepatoblasts in

*Abbreviations: Ab, antibody; AFP, α-fetoprotein; ALB, albumin; CaMKII, calcium/calmodulin-dependent kinase II; CK, cytokeratin; CPS1, carbamoyl phosphate synthetase 1; DAPI, 4′,6-diamidino-2-phenylindole; DMEM, Dulbecco's modified Eagle's medium; DMSO, dimethyl sulfoxide; E, embryonic day; EHS, Engelbreth-Holm-Swarm; FCS, fetal calf serum; Fzd, Frizzled; G6Pase, glucose 6-phosphatase; HGF, hepatocyte growth factor; HNF, hepatocyte nuclear factor; KO, knockout; mRNA, messenger RNA; MRP3, multidrug resistance–associated protein 3; NLK, Nemo-like kinase; P, postnatal day; PCNA, proliferating cell nuclear antigen; PDS, primitive ductal structure; PKC, protein kinase C; RT-PCR, reverse-transcriptase polymerase chain reaction; TAK1, transforming growth factor β–activated kinase 1; WT, wild-type.*

*From the Department of [1]Gastroenterology and Hepatology and [2]Department for Hepatitis Control, Tokyo Medical and Dental University, Tokyo, Japan; the [3]Division of Stem Cell Therapy, Institute of Medical Science, The University of Tokyo, Tokyo, Japan; the [4]Department of Gastroenterology and Hepatology, Hokkaido University, Sapporo, Japan; the [5]Department of Tissue Development and Regeneration, School of Medicine, Sapporo Medical University, Sapporo, Japan; the [6]Department of Molecular Biology and Biochemistry, Graduate School of Medicine, Osaka University, Osaka, Japan; and the [7]Institute of Innovative Science and Technology, Tokai University, Isehara, Japan.*

*Received May 11, 2012; accepted January 7, 2013.*

*This work was supported in part by Grants-in-Aid for Scientific Research from the Ministry of Education, Culture, Sports, Science and Technology in Japan; the Ministry of Health, Labor and Welfare in Japan; the Japan Society for the Promotion of Science, the Japan Health Sciences Foundation; the National Institute of Biomedical Innovation; and the Foundation for Advancement of International Science.*

**These authors contributed equally to this work.*

the fetal liver, proliferate actively and give rise to hepatocytes and cholangiocytes.[3,4] Lineage commitment of such cells can be traced by several cell surface markers, including NCAM, ICAM-1, and EpCAM in humans.[1,5] While our group[6] and others[7] demonstrated roles for transcription factors regulating the biliary differentiation of hepatic stem/progenitor cells, the molecular mechanisms behind these events have yet to be fully elucidated.

The Wnt family secreted ligands and the corresponding Frizzled family cell surface receptors play a crucial role in the differentiation, proliferation, and self-renewal of stem cells in various organs.[8] Wnt signaling pathways involve interactions between a complex set of molecular cognates that includes 19 different Wnt ligands and 10 Frizzled (Fzd) receptors in humans and mice (reviewed at http://www.stanford.edu/group/nusselab/cgi-bin/wnt/). Upon binding to Fzd receptors on the surface of a target cell, Wnt proteins activate one of two classes of downstream pathways distinguishable by their dependency on β-catenin. Examples of canonical β-catenin–dependent pathways include β-catenin–dependent activation of T cell factor by either Wnt1 or Wnt3.[8] In contrast, Wnt4 and Wnt5a activate noncanonical β-catenin–independent pathways that include downstream molecules such as calcium/calmodulin-dependent protein kinase II (CaMKII), Rho-kinase, Rac1, calcineurin, and protein kinase C (PKC).[9]

In liver development, β-catenin is known to regulate the maturation, expansion, and survival of hepatoblasts, and its deletion results in increased apoptosis of hepatoblasts in midgestational fetal livers.[10] While the function of noncanonical Wnt signaling in liver development is currently unknown, β-catenin–independent Wnt pathways have been shown to function predominantly as regulators of cell polarity and mobility in other organs.[9] In systemic Wnt5a-deficient (knockout [KO]) mice, the size of caudal structures, lung morphogenesis, and intestinal elongation are also abnormal.[11–13]

Recent reports demonstrate that Wnt5a regulates hematopoietic, mesenchymal, and neural stem cell functions.[14-16] Wnt5a has been shown to increase the repopulation of short- and long-term hematopoietic stem cells by maintaining these cells in a quiescent G0 state.[14] Wnt5a maintains mesenchymal stem cells and promotes osteoblastogenesis in preference to adipogenesis in bone marrow,[15] and also improves the differentiation and functional integration of stem cell–derived dopamine neurons.[16] In healthy adult mouse liver, Wnt5a is expressed in mature hepatocytes and cholangiocytes.[17] Nonetheless, the physiological functions of Wnt5a and the signaling cascades that it initiates during liver development and in hepatic stem/progenitor cells are unknown.

In this study, we investigated the function of Wnt5a and its downstream targets in the development of murine fetal hepatic stem/progenitor cells. Analysis of Wnt5a KO mice demonstrated that loss of Wnt5a abnormally promotes the formation of bile ductal structures in fetal liver *in vivo*. Wnt5a supplementation not only retarded the formation of bile duct–like structures, but also promoted hepatic maturation of hepatic stem/progenitor cells *in vitro*. CaMKII activity, which showed Wnt5a dependence in fetal liver, suppressed the formation of bile duct–like structures. These data indicate that Wnt5a-mediated CaMKII signaling plays an essential role in the differentiation of murine fetal hepatic stem/progenitor cells.

## Materials and Methods

***Animals.*** Systemic Wnt5a KO mice in C57BL/6 background were originally generated by Yamaguchi et al.[11] Wnt5a KO mice and wild-type (WT) littermates were produced by crossbreeding Wnt5a heterozygous mice. All animals were treated based on the guidelines of the Institute of Medical Science, University of Tokyo, and those of Tokyo Medical and Dental University.

**In Vitro *Bile Duct–Like Differentiation Assay of Primary Hepatoblasts.*** Bile duct–like differentiation assays were performed as described[6] with some modifications. Fetal hepatic cells of embryonic day (E) 14.5 liver were dissociated with collagenase,[4] and $Dlk^+$ cells were isolated from the resulting population using a magnetic cell sorter (Miltenyi Biotec, Bergisch Gladbach, Germany) and then cultured in collagen gel

*Address reprint requests to: Sei Kakinuma, M.D., Ph.D., and Mamoru Watanabe, M.D., Ph.D., Department of Gastroenterology and Hepatology, Tokyo Medical and Dental University, 1-5-45 Yushima, Bunkyo-ku, Tokyo, 1138519 Japan. E-mail: skakinuma.gast@tmd.ac.jp (S. K.) and mamoru.gast@tmd.ac.jp (M. W.); fax: (81)-3-5803-0268.*



*View this article online at wileyonlinelibrary.com.*
*DOI 10.1002/hep.26293*
*Potential conflict of interest: Nothing to report.*
*Additional Supporting Information may be found in the online version of this article.*

(Nitta Gelatin, Osaka, Japan). After 30 minutes of incubation at 37°C on basal layer collagen, 1 or 2 × $10^4$ cells were suspended in 1 mL Dulbecco's modified Eagle's medium (DMEM)/F12 mixed with 1 mL collagen gel solution and plated onto basal layer collagen in six-well culture dishes. Plated cells were cultured for 7 days with an additional 2 mL DMEM supplemented with 10% fetal calf serum (FCS) (Sigma, St. Louis, MO), 1× insulin/transferrin/selenium, 20 ng/mL epidermal growth factor (EGF, PeproTech, Rocky Hill, NJ), 20 ng/mL hepatocyte growth factor (HGF, PeproTech), and 25 ng/mL tumor necrosis factor α (PeproTech).

**In Vitro *Bile Duct–Like Differentiation Assay of Hepatic Progenitor Cell Line.*** The HPPL liver progenitor cell line has been reported to exhibit characteristics of differentiated cholangiocytes in three-dimensional culture.[18,19] As in the previous report, we maintained HPPL cells in DMEM/F12 containing 10% FCS, 1× insulin/transferrin/selenium, 10 mM nicotinamide, $10^{-7}$ M Dex, and 5 ng/mL HGF and EGF and suspended cells in a mixture of type I collagen and Engelbreth-Holm-Swarm (EHS) sarcoma gel (Becton Dickinson, Bedford, MA) at a density of 4 × $10^4$ cells/mL. Cell suspension was added to each cell culture insert (Millipore, Billerica, MA) and after incubation at 37°C for 2 hours, 500 μL of DMEM/F12 with growth factors was added above and below the insert, and the cells were cultured for 7 days. To test the effects of inhibitors of CaMKII, Rho-kinase, Rac1, calcineurin, and PKC on HPPL differentiation, KN93, KN92, KN62, Y-27632, NSC23766, cyclosporin A, and Go6976 (Supporting Information) were added individually to the culture medium when each three-dimensional culture was initiated. Independent analyses were performed in triplicate, and five fields were randomly selected for counting the cysts that indicate bile duct–like differentiation of cells.

**In Vitro *Hepatic Maturation Assay of Primary Hepatoblasts.*** To induce hepatic differentiation, primary hepatoblasts from WT E14.5 mice were cultured as described.[6] Briefly, 2.5 × $10^5$ magnetic cell sorter–isolated $Dlk^+$ cells were cultured in DMEM supplemented with 10% FCS, 2 mM L-glutamine, 1× nonessential amino acid, 100 U/mL penicillin, 100 μg/mL streptomycin, and $10^{-7}$ M Dex in each well of a six-well gelatin-coated dish. After 5 days, the resulting cells were supplemented with medium containing 20% EHS gel for an additional 2 days prior to analysis.

Details regarding materials, cell isolation, hematoxylin and eosin staining, reverse-transcriptase polymerase chain reaction (RT-PCR) analysis, immunostaining, immunoblot analysis, Wnt5a-blocking experiments, microarray analysis, and statistical analysis are described in the Supporting Information.

## Results

***Expressions of Wnt5a and Frizzled Receptors During Liver Development.*** We first analyzed *Wnt5a* expression during liver development using quantitative RT-PCR. *Wnt5a* expression was detected in fetal and neonatal livers of WT mice and showed a gradual increase during liver development (Fig. 1A). To investigate Wnt5a expression in midgestational fetal liver, we purified the fractions of hepatoblasts, mesenchymal cells, mesothelial cells, endothelial cells, and hematopoietic cells from E14.5 liver using FACS. Quantitative RT-PCR analysis indicated that *Wnt5a* was expressed in hepatoblasts, mesenchymal cells, mesothelial cells, endothelial cells, and hematopoietic cells. The expression level of Wnt5a was significantly higher in mesenchymal cells than in hepatoblasts and other types of cells in midgestational fetal liver (Fig. 1B). Frizzled is a family of cell surface receptors for Wnt ligands. Adult hepatocytes from 12-week-old mice served as the control. RT-PCR analysis of E14.5 hepatoblasts resulted in the detection of 9 of 10 Fzd receptors (all except *Fzd9*), whereas E14.5 hematopoietic cells expressed 9 of 10 Fzd receptors (all except *Fzd2*) (Fig. 1C and Supporting Fig. 1).

***Loss of Wnt5a Promotes the Formation of Bile Duct in Fetal Liver.*** Because one of the reported phenotypes of systemic Wnt5a KO mice was postpartum death,[11] we investigated the function of Wnt5a in liver development using mid- to late gestational fetuses. We determined that although average liver weight in Wnt5a KO E18.5 fetal mice was significantly lower than in WT littermates, the average liver/body weight ratio in KO mice was not significantly different from the ratio in WT mice (Supporting Fig. 2).

Histological analysis of E18.5 livers showed that the number of luminal spaces around the portal vein, which we interpret to be primitive bile ducts, was greater in Wnt5a KO mice than in WT mice (Fig. 2A). To further investigate these changes in bile duct development, expression of *Sox9* (a representative transcriptional factor expressed in biliary precursor cells)[20] was analyzed. Expression levels of *Sox9* were significantly higher in Wnt5a KO E16.5 fetal livers relative to WT livers (Fig. 2B). The Notch pathway plays an essential role in the morphogenesis of bile duct structures.[21] Expression levels of *Notch1*, *Notch2*, and

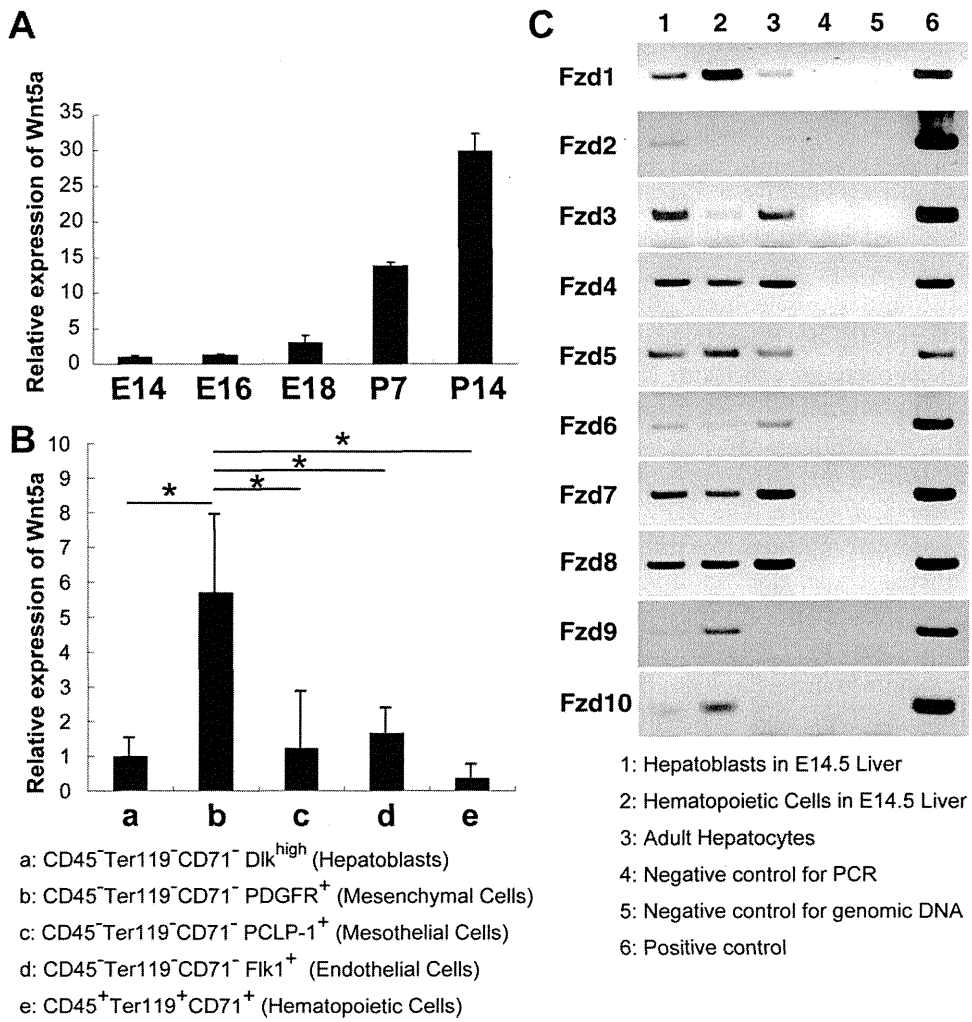


Fig. 1. Expression analyses of Wnt5a and Fzd receptors during liver development. (A) Quantitative RT-PCR analysis of Wnt5a in fetal and neonatal livers. E14, E16, E18, P7, and P14 indicate Wnt5a expression in whole livers derived from WT mice at these days of development, respectively. Values represent the ratio of Wnt5a at each stage relative to expression of this RNA in E14.5 fetal liver following normalization of template copy number to $\beta$-actin. Bars represent the mean ± SD of three separate experiments. (B) Quantitative RT-PCR analysis of Wnt5a. Lane a: $CD45^-Ter119^-CD71^-Dlk^{high}$ cells from E14.5 liver (hepatoblasts). Lane b: $CD45^-Ter119^-CD71^-PDGFR^+$ cells from E14.5 liver (mesenchymal cells). Lane c: $CD45^-Ter119^-CD71^-PCLP\text{-}1^+$ cells from E14.5 liver (mesothelial cells). Lane d: $CD45^-Ter119^-CD71^-Flk1^+$ cells from E14.5 liver (endothelial cells). Lane e: $CD45^+Ter119^+CD71^+$ cells from E14.5 liver (hematopoietic cells). All lanes were normalized by numbers of $\beta$-actin copies quantified by TaqMan-PCR analysis; equal numbers of copies were applied as templates. Wnt5a expression was significantly higher in mesenchymal cells than in hepatoblasts, mesothelial cells, endothelial cells and hematopoietic cells. Bars represent the mean ± SD of three separate experiments. *$P < 0.05$. (C) Expression of Fzd family. Lane 1: hepatoblasts ($CD45^-Ter119^-Dlk^{high}$ cells) purified from E14.5 liver. Lane 2: hematopoietic cells ($CD45^+Ter119^+$ cells) from E14.5 liver. Lane 3: adult hepatocytes from 12-week-old mouse liver. Lane 4: negative control (distilled water). Lane 5: samples without reverse-transcriptase reaction (negative controls for false-positive amplification of genomic DNA). Lane 6: positive control. RT-PCR products of Fzd receptors are indicated. Images shown are representative of three separate experiments.

*Jagged1* were significantly higher in Wnt5a KO E16.5 fetal livers relative to WT livers (Supporting Fig. 3A). Numbers of $Hes1^+$ cells in E18.5 livers were significantly greater in Wnt5a KO mice than in WT mice (Supporting Fig. 3B). Expression levels of *Cyclin D1* and *c-Myc* (target transcripts of canonical $\beta$-catenin–dependent Wnt pathway) in Wnt5a KO livers were equal to those in WT livers (Supporting Fig. 4A). We tried to assess the protein level of Sox9; however, immunostaining analysis of Sox9 did not work well, probably due to technical problems (data not shown).

During normal liver development, hepatoblasts located around the portal vein develop as hepatocyte nuclear factor (HNF) $1\beta^+HNF4\alpha^-$ biliary precursor cells.[22] In normal E16.5 fetal livers, monolayer rings of biliary precursor cells, termed ductal plates, can be detected.[23] WT E18.5 fetal livers contained primitive ductal structures (PDSs) consisting of multiple $HNF1\beta^+$ cytokeratin $(CK)19^+$-cell lumina (Fig. 2C).

Immunohistological analysis revealed that numbers of $HNF1\beta^+HNF4\alpha^-$ biliary precursor cells in E16.5 livers (Fig. 2D) and in PDSs formed by these cells in

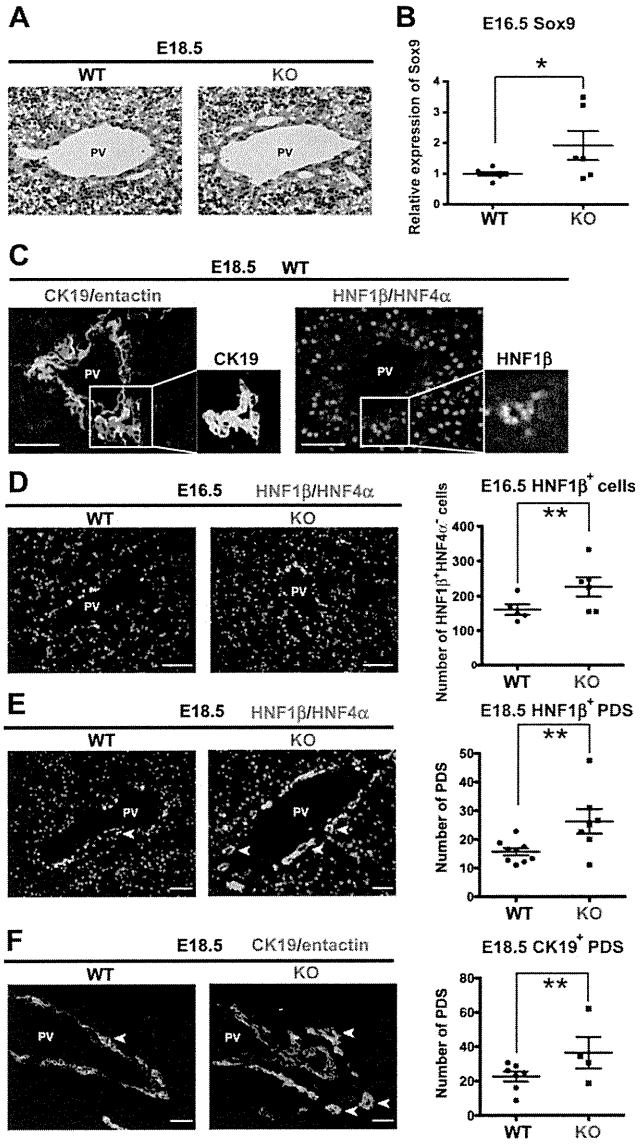


Fig. 2. Loss of Wnt5a excessively promotes the formation of bile duct in fetal liver. (A) Representative images depicting luminal spaces around the portal vein (PV) in E18.5 Wnt5a KO and littermate WT livers stained with hematoxylin and eosin. (B) Quantitative RT-PCR analysis of the cholangiocyte marker Sox9 is depicted as the ratio of Sox9 copy number in E16.5 Wnt5a KO livers relative to WT livers (all normalized to $\beta$-actin). Steady-state levels of Sox9 mRNA were significantly higher in Wnt5a KO livers relative to WT livers. $^*P < 0.05$. (C) Representative images of immunostained sections from E18.5 WT livers. Left panel: double immunostaining using CK19 (red) and entactin (green) antibodies. Right panel: double immunostaining using HNF1$\beta$ (green) and HNF4$\alpha$ (red) antibodies. Insets depict high-power field images of cells with positive staining for CK19 (left panel) and HNF1$\beta$ (right panel). PV, portal vein. (D, E) Left two panels: immunostaining of HNF1$\beta$ (green) and HNF4$\alpha$ (red) in E16.5 (D) and E18.5 (E) livers. Right panel (D): number of HNF1$\beta^+$HNF4$\alpha^-$ cells in 10 random fields examined in WT and Wnt5a KO livers. Right panel (E): number of primitive ductal structures (PDSs) in 10 random fields examined in WT and Wnt5a KO livers. PV, portal vein. (F) Left panel: immunostaining of CK19 (red) and entactin (green) in E18.5 livers. Right panel: numbers of PDSs in 10 random fields of WT and Wnt5a KO livers. Arrowheads indicate PDSs. PV, portal vein. Images shown are representative of three independent experiments. Bars in dot-plot graphs represent mean ± SEM of values shown. $^{**}P < 0.01$. Scale bars: 50 $\mu$m.

E18.5 livers (Fig. 2E) were significantly higher in Wnt5a KO mice relative to WT mice. Double staining of CK19 and entactin (a component of basement membrane) confirmed that the number of PDSs formed by CK19$^+$ cells was also significantly higher in E18.5 Wnt5a KO liver relative to WT liver (Fig. 2F). These results demonstrate clearly that loss of Wnt5a excessively promotes the formation of bile ducts in fetal liver.

***Expression Analysis of Fetal Livers in Wnt5a KO Mice.*** Expression of genes coincident with hepatic maturation was also analyzed in Wnt5a KO fetal livers using quantitative RT-PCR. In E16.5 fetal livers, albumin (ALB) and HNF4$\alpha$ messenger RNA (mRNA) levels were nearly equal between WT and Wnt5a KO mice. Similarly, we observed no significant differences between WT and Wnt5a KO E18.5 fetal livers with regard to copy numbers of tyrosine aminotransferase, carbamoyl phosphate synthetase 1 (CPS1), glucose 6-phosphatase (G6Pase), or HNF4$\alpha$ mRNAs (Supporting Figs. 5A and B). These data suggest that the maturation of hepatoblasts to hepatocytes is not impaired in Wnt5a KO mice.

Proliferation of fetal liver cells in Wnt5a KO mice was analyzed by immunoblot and immunostaining. Immunoblot analysis revealed that proliferating cell nuclear antigen (PCNA) production in Wnt5a KO livers was almost equal to that in WT livers (Supporting Fig. 4B). Numbers of CK19$^+$PCNA$^+$ cells in E18.5 were almost equal to those in WT livers (Supporting Fig. 4C). Changes in gene expression in Wnt5a KO livers were analyzed using complementary DNA microarray analysis (Supporting Fig. 5C and Supporting Table 5). Cluster analysis revealed that several molecules associated with amino acid metabolism and cell migration were up-regulated or down-regulated in Wnt5a KO fetal livers compared with those in WT livers.

***Wnt5a Retards Formation of Bile Duct–Like Structures from Primary Hepatoblasts.*** In collagen gel-embedding culture, mouse primary hepatoblasts differentiate into bile duct–like branching structures, coincident with the expression of biliary cell-specific genes such as CK19 (Fig. 3A, left panel).[6] To investigate the effects of Wnt5a on differentiation of hepatoblasts into biliary cells *in vitro*, we cultured primary hepatoblasts derived from E14.5 WT fetal livers and assessed the formation of bile duct–like branching structures.

We observed that cells in cultures derived from E14.5 WT fetal liver formed approximately 10 colonies (consisting of >100 cells in large branching structures) per $1 \times 10^4$ cells (Fig. 3A, right panel); colonies with

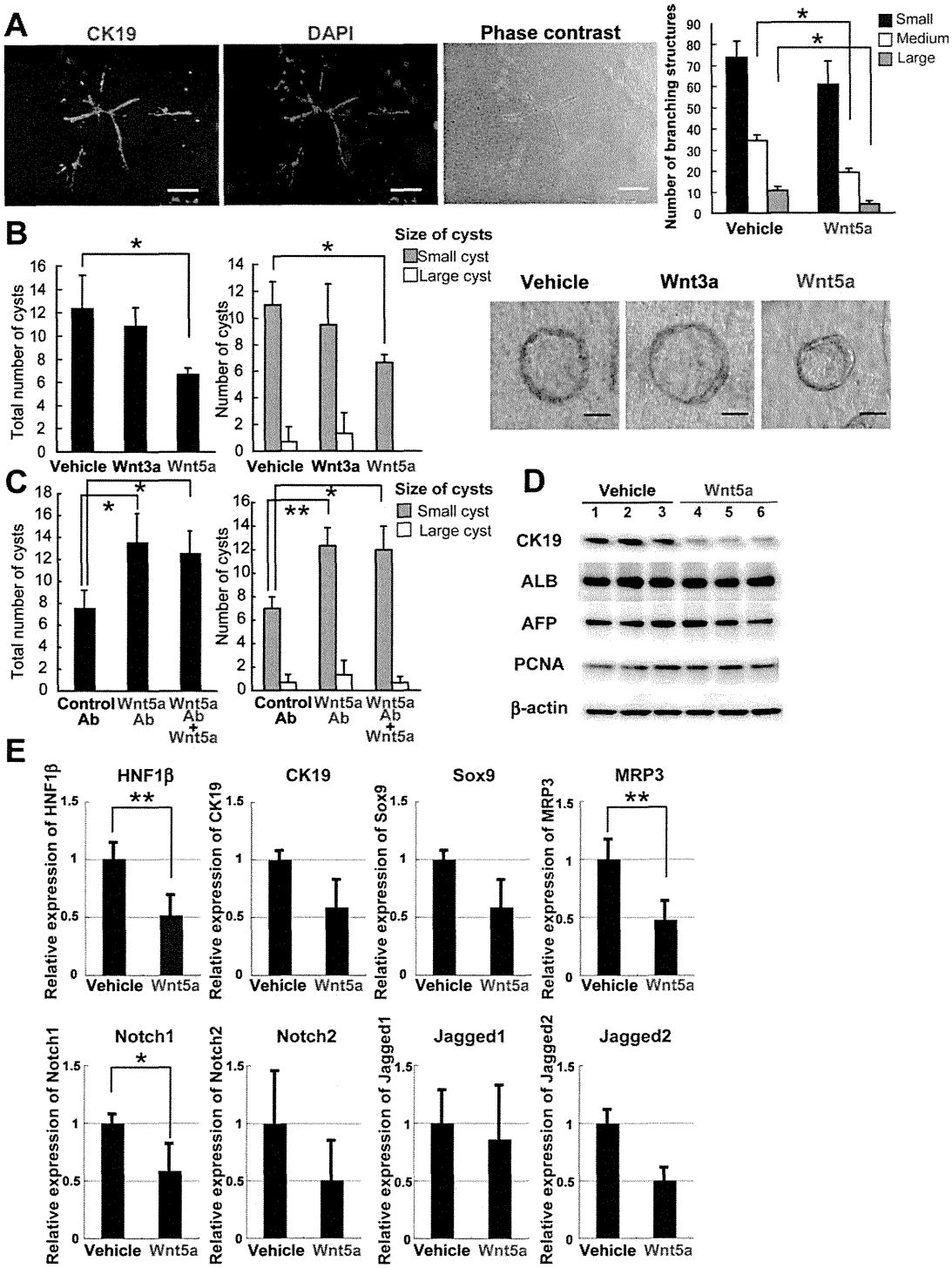


Fig. 3. Wnt5a suppresses formation of bile duct-like structures derived from hepatic stem/progenitor cells. (A) Bile duct-like branching structures derived from primary hepatoblasts. Left panel: representative view of bile duct-like branching structures consisting of >100 cells derived from primary hepatoblasts. Colonies were immunostained with CK19 (green) and counterstained with 4',6-diamidino-2-phenylindole (DAPI) (blue). Scale bar: 100 $\mu$m. Right panel: numbers of colonies demonstrating branching structures in cultures supplemented with 100 ng/mL Wnt5a or vehicle only. Numbers of small (consisting of 10-49 cells), medium-sized (50-99 cells), and large (>100 cells) branching structures per one well were counted. *$P < 0.05$. (B) Numbers of bile duct-like cysts derived from the hepatic stem/progenitor cell line (HPPL) in five random fields per well in cultures supplemented with 100 ng/mL Wnt5a, 100 ng/mL Wnt3a, or vehicle only (left panel). There were significantly fewer small cysts (50-100 $\mu$m diameter with clear lumina) and large cysts (diameter >100 $\mu$m with clear lumina) in cultures supplemented with Wnt5a relative to vehicle only. Right panel: representative views of cysts in HPPL three-dimensional cultures supplemented with either vehicle, Wnt3a or Wnt5a. Scale bars: 50 $\mu$m. *$P < 0.05$. (C) Numbers of bile duct-like cysts derived from HPPL in five random fields per well in cultures supplemented with either control immunoglobulin G, anti-Wnt5a Ab, or both anti-Wnt5a Ab plus recombinant Wnt5a protein. Cultures treated with anti-Wnt5a Ab resulted in a significant increase in total numbers of bile duct-like cysts derived from HPPL, and blocked the effect of Wnt5a supplementation. *$P < 0.05$. **$P < 0.01$. (D) Immunoblot analysis of CK19, ALB, AFP, and PCNA in HPPL-derived cysts treated with Wnt5a. CK19 production in HPPL-derived cysts treated with Wnt5a was down-regulated relative to that with vehicle-supplemented controls, whereas protein levels of ALB, AFP, and PCNA did not change. Lanes 1-3 and lanes 4-6 are vehicle-supplemented controls and Wnt5a-supplemented HPPL-derived cysts, respectively. (E) Expression analysis of HPPL-derived cysts treated with Wnt5a. Expression levels of HNF1$\beta$, MRP3, and Notch1 in HPPL-derived cysts in medium supplemented with Wnt5a were significantly lower than those in HPPL-derived cysts in medium supplemented with vehicle, indicating that Wnt5a retarded biliary maturation of HPPL cysts. Results represent the mean ± SD of three separate experiments. *$P < 0.05$. **$P < 0.01$.

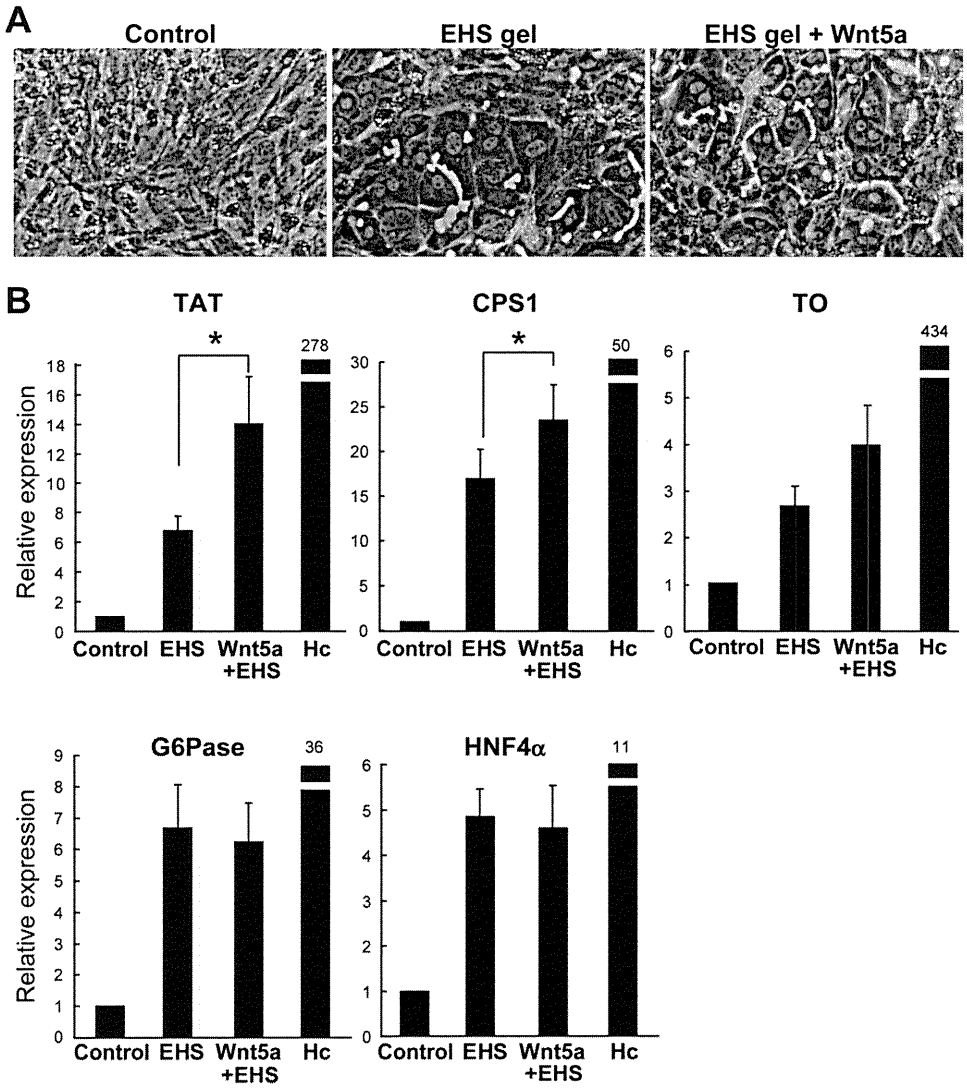


Fig. 4. Expression of hepatic maturation markers under culture supplemented with Wnt5a. (A) Phase contrast images of cultured primary hepatoblasts induced to mature to hepatocytes with EHS gel alone or EHS gel plus 100 ng/mL Wnt5a. (B) Expression levels of tyrosine amino transferase (TAT), CPS1, tryptophan-2,3-oxygenase (TO), G6Pase, and HNF4α are depicted as the ratio of copy mRNA number in cells treated with EHS gel alone or EHS gel plus 100 ng/mL Wnt5a for 7 days relative to control cells. Hc, primary adult hepatocytes from 12-week-old mice (positive control). All samples were normalized by numbers of β-actin copies quantified by TaqMan-PCR analysis; equal numbers of copies were applied as templates. Results represent the mean ± SD of three independent experiments. $*P < 0.05$.

medium (50-99 cells) or small (10-49 cells) branching structures also were noted. In cultures supplemented with Wnt5a, there were significant decreases in the average number colonies with large- and medium-sized branching structures relative to vehicle-only controls.

***Wnt5a Suppresses Cyst Formation Derived from HPPL in Three-Dimensional Culture.*** To assess the potential of hepatic stem/progenitor cells for bile duct–like luminal formation, we used an HPPL three-dimensional culture system.[19] HPPL is established from mouse E14 $Dlk^+$ hepatoblasts and differentiates into hepatic and cholangiocytic lineages.[18] In this system, HPPL cells form cysts that exhibit characteristics of differentiated cholangiocytes producing CK19, E-cadherin, and other characteristic markers. We categorized HPPL-derived colonies into one of three classes: colonies without clear lumina, small cysts (50-100 μm diameter with clear lumina), and large cysts (>100 μm diameter with clear lumina). As described,[19] immuno-cytostaining of cultured cells showed that colonies without clear lumina produced both the hepatic marker ALB and the biliary marker CK19, suggesting incomplete terminal differentiation. Cells in the luminal walls of small and large cysts, in contrast, produced CK19 but not ALB, indicating their differentiation to a cholangiocyte lineage (Supporting Fig. 6). Vehicle-only controls or cultures treated with Wnt3a did not show a significant difference in overall number of cysts. In contrast, cultures supplemented with Wnt5a displayed significantly fewer cysts, due both to an absence of large cysts and a significantly reduced number of small cysts (Fig. 3B). Wnt5a is expressed in HPPL cells (Supporting Fig. 7A). We verified the specificity of effect of Wnt5a by blocking experiments. Cultures supplemented with anti-Wnt5a antibody (Ab) resulted in a significant increase in numbers of HPPL-derived cysts relative to control Ab, and

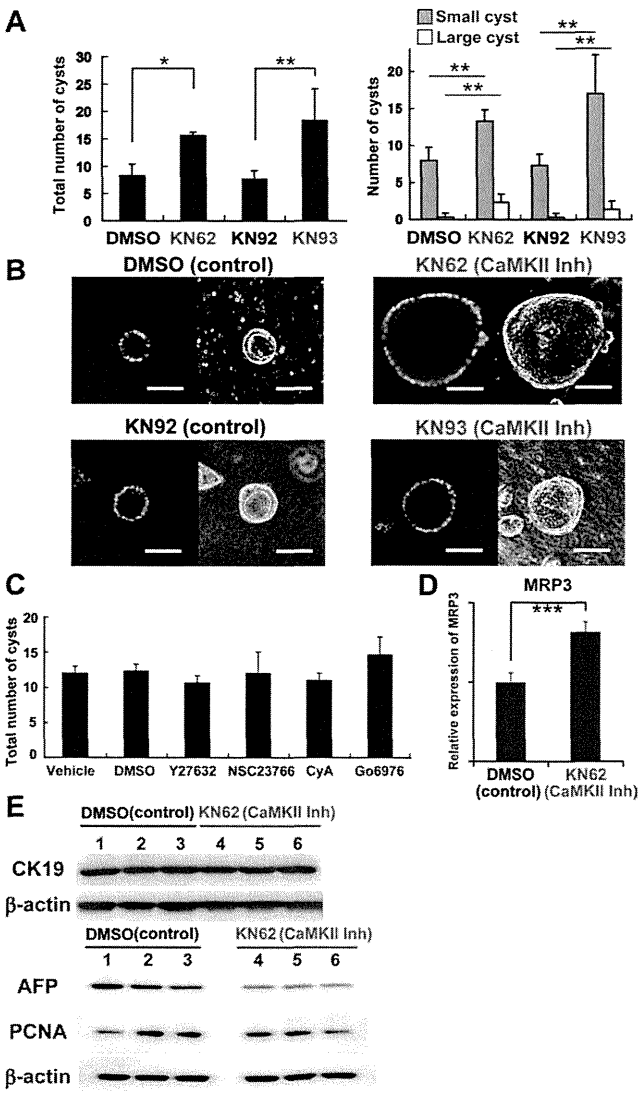


Fig. 5. Inhibitors of CaMKII increased the number and size of bile duct-like cysts derived from HPPL. (A) Inhibitors specific for CaMKII activity (KN62 and KN 93) were added at the beginning of HPPL three-dimensional culture. Numbers of total cysts, small cysts, and large cysts increased significantly in medium supplemented with KN62 or KN93. Cultures treated with dimethyl sulfoxide (DMSO) alone (vehicle) or KN92 (an inactive analogue of KN93) served as negative controls for KN62 (vehicle) and KN93, respectively. $*P < 0.01$. $**P < 0.05$. (B) Representative DAPI-stained (blue, left panels) or phase contrast confocal microscopy images (right panels) of bile duct-like cysts. Scale bars: 100 $\mu$m. (C) Numbers of total cysts were not changed by the inhibitors of Rho kinase (Y-27632), Rac1 (NSC23766), calcineurin (cyclosporin A [CyA]), or PKC (Go6976). Vehicle-only treatments (distilled water or DMSO) served as negative controls for Y-27632 (in distilled water), NSC23766 (in distilled water), CyA (in DMSO), and Go6976 (in DMSO). (D) Expression of MRP3 in HPPL cysts. MRP3 expression was significantly increased in medium supplemented with CaMKII inhibitor (KN62), suggesting that CaMKII inhibitor promoted biliary maturation of HPPL cysts. $***P < 0.01$. (E) Immunoblot analysis of CK19, AFP, and PCNA in HPPL-derived cysts treated with vehicle (DMSO) or CaMKII inhibitor (KN62). The level of AFP in HPPL-derived cysts treated with CaMKII inhibitor was lower than that in vehicle-supplemented controls, whereas the levels of CK19 and PCNA did not change. Results represent the mean ± SD of three independent experiments.

blocked the effects of Wnt5a supplementation (Fig. 3C). Numbers of HPPL-derived cysts were higher in cultures supplemented with Wnt5a-specific inhibitor relative to vehicle-only controls (Supporting Fig. 7B).

Immunoblot analysis indicated that CK19 production in HPPL-derived colonies were significantly down-regulated in cultured cells supplemented with Wnt5a relative to vehicle-supplemented controls, whereas the levels of ALB, $\alpha$-fetoprotein (AFP), and PCNA did not change (Fig. 3D). Expression analysis of HPPL-derived colonies revealed that HNF1$\beta$, Notch1, and multidrug resistance–associated protein 3 (MRP3, a key primary active transporter in biliary cells) were significantly down-regulated in cultured cells supplemented with Wnt5a relative to vehicle-supplemented controls (Fig. 3E). HNF1$\beta$ and Sox9 were significantly up-regulated in cultured cells supplemented with anti-Wnt5a Ab relative to control Ab (Supporting Fig. 7C), whereas the levels of hepatocytic markers did not change (Supporting Fig. 7D). Consistent with our *in vivo* results, these data indicate that Wnt5a suppresses bile duct–like cyst formation of fetal hepatic progenitor cells *in vitro*.

***Wnt5a Induces the Expression of Hepatic Maturation Markers in Primary Hepatoblasts* In Vitro.** We evaluated the potential of primary hepatoblasts for hepatic maturation using an *in vitro* hepatic differentiation assay.[24] Phase-contrast microscopy after addition of EHS gel identified several morphological changes within cells, including formation of highly condensed cytosol, and clear, round nuclei typical to mature hepatocytes (Fig. 4A, middle panel). Because similar gross morphological changes were also seen in cells cultured in the presence of Wnt5a (right panel), we used quantitative RT-PCR to measure the effect of Wnt5a on expression of hepatic maturation marker genes in stem/progenitor cells. Expression of tyrosine aminotransferase and CPS1 in cultured cells increased significantly with supplemental Wnt5a (Fig. 4B), whereas changes in tryptophan-2,3-dioxygenase, G6Pase, and HNF4$\alpha$ mRNA levels were not significantly different. These results indicate that Wnt5a contributes, in part, to primary hepatoblast maturation. Taken together, our *in vitro* data demonstrate that Wnt5a retards biliary differentiation and promotes hepatic differentiation of hepatoblasts.

***Inhibition of CaMKII Activity Promotes the Formation of Bile Duct–Like Cysts Derived from HPPL.*** While Wnt5a is known to stimulate several signaling cascades, including CaMKII, Rho-kinase, Rac1, calcineurin, and PKC, the specific cascade triggered by Wnt5a in hepatic stem/progenitor cells is unknown. To address this question, we analyzed the effects of specific